5

The South American Monsoon System: Climatology and Variability

Viviane B. S. Silva and Vernon E. Kousky
NOAA/National Weather Service
Climate Services Division
Climate Prediction Center
USA

1. Introduction

A typical Monsoon System is characterized by a reversal in the low-level wind direction between summer and winter seasons, and distinct wet (summer) and dry (winter) periods. The changes in low-level atmospheric circulation are related to changes in the thermal contrast between oceans and continents. During summer, the air over continents is warmer and more convectively unstable than air over adjacent oceanic regions. Consequently, lower pressure occurs over land and higher pressure occurs over nearby oceanic areas. This pressure pattern causes low-level moist air to converge onto the land, resulting in precipitation, especially during the late afternoon and evening hours. During winter the temperature contrasts and low-level atmospheric circulation are reversed, resulting in dry conditions over continents.

The regions on the globe that show distinct monsoon characteristics include 1) western Sub-Saharan Africa, 2) Asia (India, southern China, Korea and parts of Japan), 3) Northern Australia, 4) South America (Brazil, Bolivia, Paraguay) and 4) North America (Southern US and Mexico). The focus of this chapter is on the South American Monsoon System (SAMS).

South America has several important geographical features that contribute to the climate of the region (Fig. 1). The entire continent is surrounded by water, with the high Andes Mountains stretching along the entire west coast. South America also contains the world's largest rainforest (the Amazon) and driest Desert (Atacama in Chile). The core of the SAMS includes the Brazilian "Planalto" (BP), which contains the headwaters of major rivers flowing into the Amazon, La Plata and São Francisco basins. Those basins contain major agricultural areas and provide most of Brazil's hydroelectric energy production.

The SAMS displays considerable variability on time scales ranging from diurnal to inter-annual. Prolonged periods of wetter-than-average or drier-than-average conditions can have significant impacts on agriculture, energy production, and society in general. Due to the accentuated topography near Brazil's east coast, heavy rainfall can result in disastrous flooding, with loss of life, property and infrastructure. In many cases, the poorest inhabitants suffer the greatest impacts from heavy rainfall events, since they often reside in

the most vulnerable areas, such as along streams and on steep unstable slopes. In addition, persistent rainfall deficits (droughts) can have negative impacts on agriculture and also on Brazil's energy production, leading to restrictions on energy usage affecting large sections of Brazil (e.g., Silva et al., 2005).

Fig. 1. South American key topographic features and major river basins [Amazon basin (light yellow), Sao Francisco basin (light green) and La Plata basin (light blue)]. The Brazilian "Planalto" (BP) is indicated by the red oval.

The objective of this chapter is to provide an overview of 1) the characteristic features of SAMS, including the evolution of precipitation and atmospheric circulation during the wet season, 2) the variability of SAMS on time scales ranging from diurnal to inter-annual, and 3) extreme rainfall events and their impacts.

2. Data sets

Precipitation data used to show the characteristic features of SAMS are derived from gridded daily precipitation analyses available from the NOAA/Climate Prediction Center (Silva et al., 2007; Chen et al., 2008). Prior to selecting a data set as the basis for an analysis of mean circulation features, an inter-comparison among six re-analyses was made for South America during the period 1979-2000. The selected re-analyses for comparison are: the NCEP/Climate Forecast System Reanalysis (CFSR) (Saha et al., 2010), the NCEP/NCAR CDAS-Reanalysis (R1) (Kalnay et al., 1996), the NCEP/Department of Energy-DOE Reanalysis (R2) (Kanamitsu et al., 2002), the European Centre for Medium-Range Forecasts (ECMWF) Reanalysis (ERA-40) (Uppala et al., 2005), the NASA /Global Modeling and Assimilation Office (GMAO) Reanalysis (MERRA) (Rienecker et al., 2011), and the Japanese Meteorological Agency Reanalysis (JRA-25) (Onogi, et al., 2005, 2007).

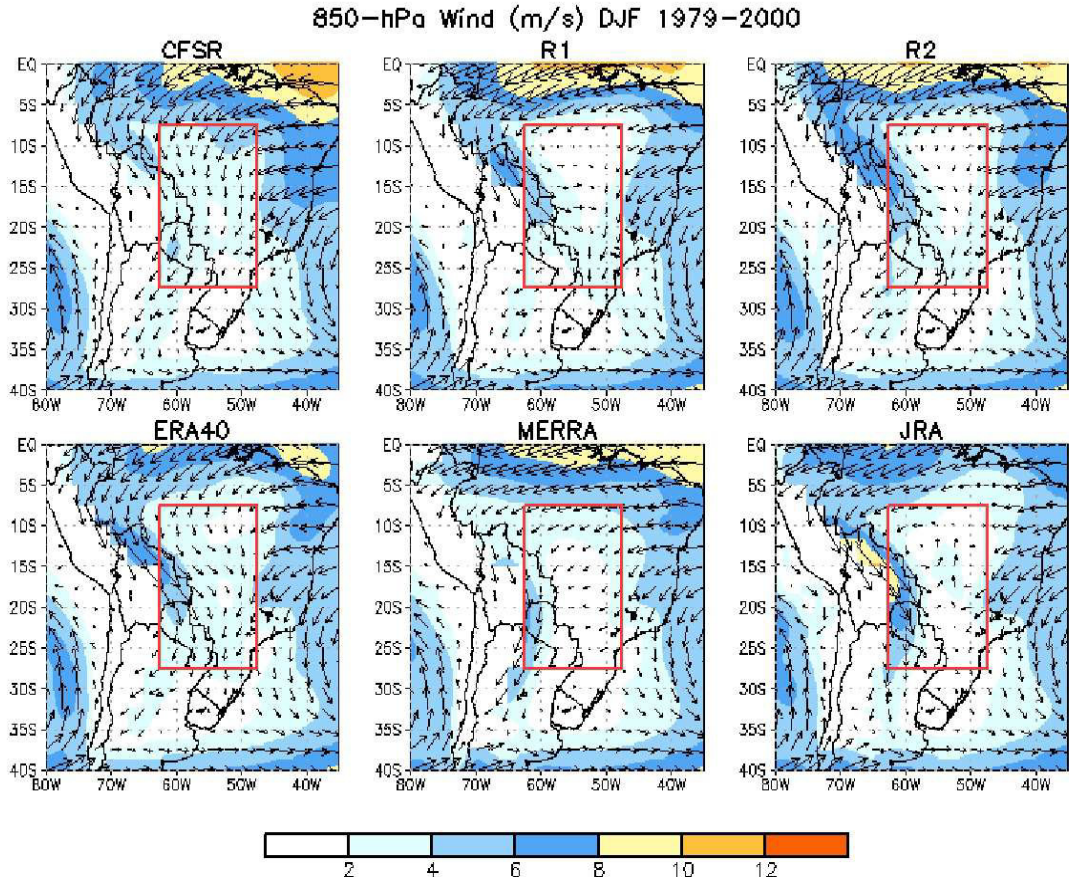

Fig. 2. Mean 850-hPa wind direction (vectors) and magnitude (shading, ms^{-1}) taken from six reanalysis data sets for December-February 1979-2000.

The upper-tropospheric circulation (200-hPa wind, not shown) is in good agreement among the various re-analyses over the entire region. Therefore, any of the reanalysis data sets could be used to qualitatively describe upper-tropospheric circulation features. In contrast, the December-February (DJF) mean (1979-2000) lower-tropospheric circulation (850-hPa wind) shows considerable variability among the re-analyses in the orientation and strength of the low-level flow (low-level jet) east of the Andes within the area 7.5º-20ºS, 45º-65ºW (red boxes in Fig. 2). Consequently, there is considerable uncertainty in the analyzed low-level flow characteristics in this region and in derived quantities, such as moisture flux, convergence, and vertical motion within the core region of the SAMS.

Comparing the DJF 1979-2000 mean precipitation patterns in the re-analyses to the analyzed station-based precipitation (Fig. 3) it is evident that the CFSR pattern is more similar to the observation-based pattern [lower right panel - OI (T62)] than any of the other reanalysis patterns. CFSR improvements include the proper location of a maximum in precipitation over the southern Amazon basin, and an absence of the spurious maximum over northeastern Brazil that is evident in the other reanalysis patterns. Silva et al., 2011 found that the pattern correlation between the DJF CFSR mean precipitation pattern and the observed precipitation pattern is much higher for CFSR than for either R1 or R2.

Furthermore, the DJF CFSR 500-hPa mean vertical motion pattern is much better correlated with the observed precipitation pattern than are the 500-hPa vertical motion patterns in R1 and R2 (Silva et al., 2011). Consequently, in the remainder of this chapter we will use the CFSR data to describe the mean circulation features related to SAMS. R1 analyses will be used in a qualitative manner to describe features related to extreme events.

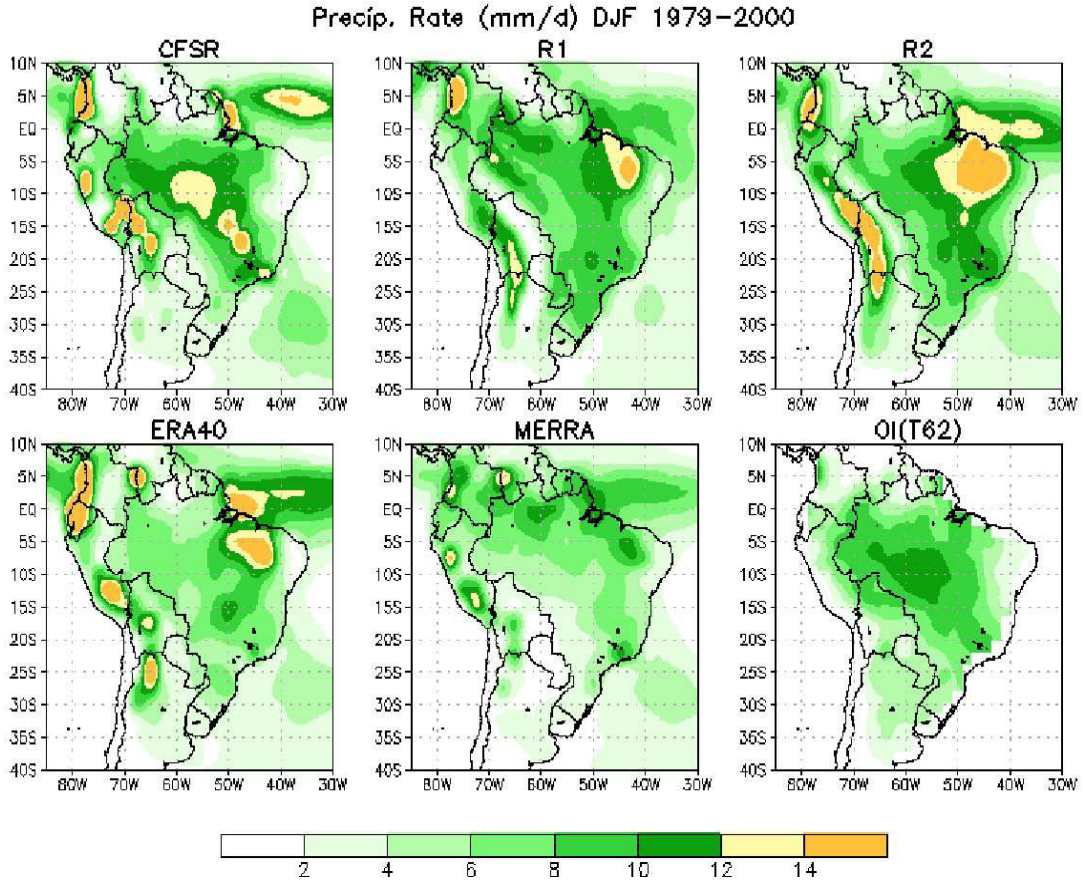

Fig. 3. Mean precipitation (mm d^{-1}) from five reanalysis data sets, and a station-based analysis (OI-T62, lower right panel) for December-February 1979-2000.

3. Characteristic features of SAMS

3.1 Major large-scale elements affecting the South American Monsoon System

The South American Monsoon System (SAMS) has been a major focus of the CLIVAR/VAMOS (Variability of the American Monsoon System) program. [CLIVAR is the World Climate Research Programme (WCRP) project that addresses Climate Variability and Predictability, with a particular focus on the role of ocean-atmosphere interactions in climate]. Several studies and reviews on the SAMS have described major features and phenomena that affect the behavior of SAMS on various time scales (e.g., Gan et al., 2004; Grimm et al., 2005; Vera at al., 2006; Gan et al., 2009; Liebmann & Mechoso, 2010; Marengo et al., 2010). The CLIVAR/VAMOS Panel developed a schematic diagram showing the major large-scale features related to the South American Monsoon System (Fig. 4). The

Andes mountains and Amazon basin play important roles in the South America monsoon. The Andes act as a barrier to the low-level easterly flow, which is deflected to the south over western Brazil, Bolivia and Paraguay during the austral summer. Intense summertime convection and latent heating over the continent contribute to the formation of an upper-tropospheric anticyclone, often referred to as the "Bolivian High". The rising air motion over the continent is compensated by sinking motion over the adjacent Pacific and Atlantic Oceans. These oceanic regions feature an absence of deep convection and the presence of upper-tropospheric cyclonic circulation (troughs).

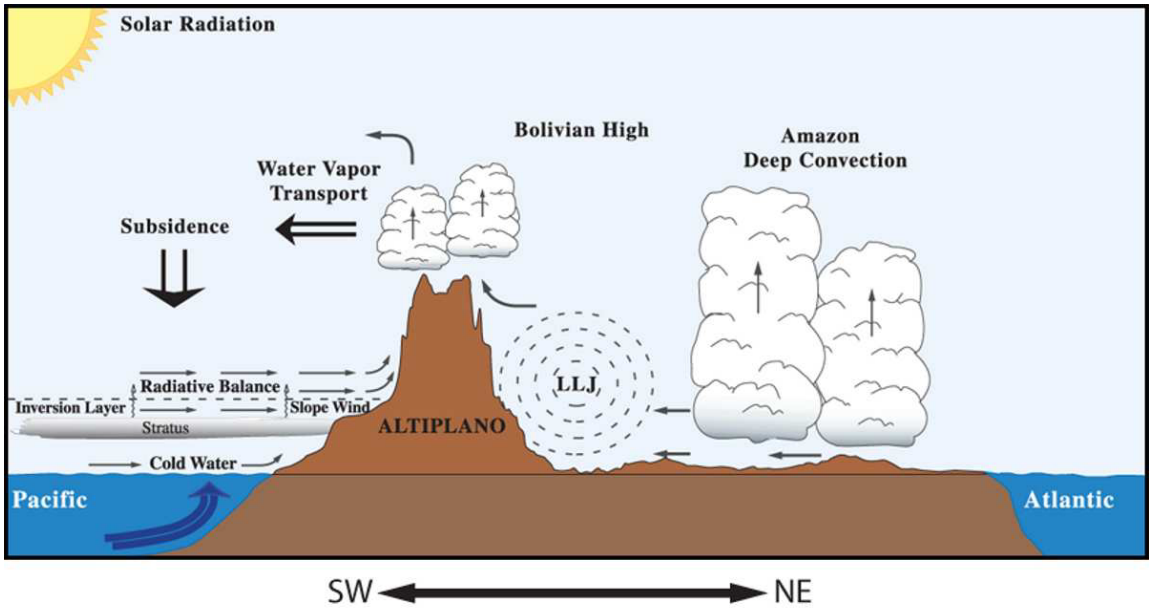

Fig. 4. Section across South America displaying schematically the major large-scale elements related to the South American Monsoon System. Source: Climate Variability & Predictability Program (CLIVAR)
(http://www.clivar.com/publications/other_pubs/clivar_transp/pdf_files/av_g3_0106.pdf)

3.2 Life cycle of the SAMS wet season

The annual cycle of precipitation, over tropical South America, features distinct wet and dry seasons between the equator and 25ºS. Portions of central and eastern Brazil and the Andes Mountains between 12ºS and 32ºS receive more than 50% of their total observed annual precipitation during the austral summer (December-February: DJF) (Fig. 5). These same regions receive less than 5% of their total annual precipitation during the austral winter (June-August: JJA). The area from the mouth of the Amazon River to northern Northeast Brazil experiences a maximum in precipitation during austral fall (March-May: MAM).

During the wet season an upper-tropospheric anticyclone dominates the circulation over tropical and subtropical South America, while cyclonic circulation dominates the upper-tropospheric circulation over low latitudes of the eastern South Pacific and central South Atlantic (Fig. 6, top panel). The position of the upper-level anticyclone (southwest of the region of most intense precipitation and latent heating) is consistent with the atmospheric circulation response to tropical forcing (heating) (e.g., Webster 1972; Gill 1980). Prominent

low-level features (Fig. 6, bottom panel) include: 1) surface high pressure systems and anticyclonic circulation over the subtropical oceans (Pacific and Atlantic), 2) a surface low-pressure system (Chaco Low) centered over northern Argentina, and 3) a low-level northwesterly flow (low-level jet) extending from the southwestern Amazon to Paraguay and northern Argentina. Throughout the region one notes a reversal of circulation features between the lower troposphere and the upper troposphere (Fig. 6, compare bottom and top panels), which is typical of the global Tropics.

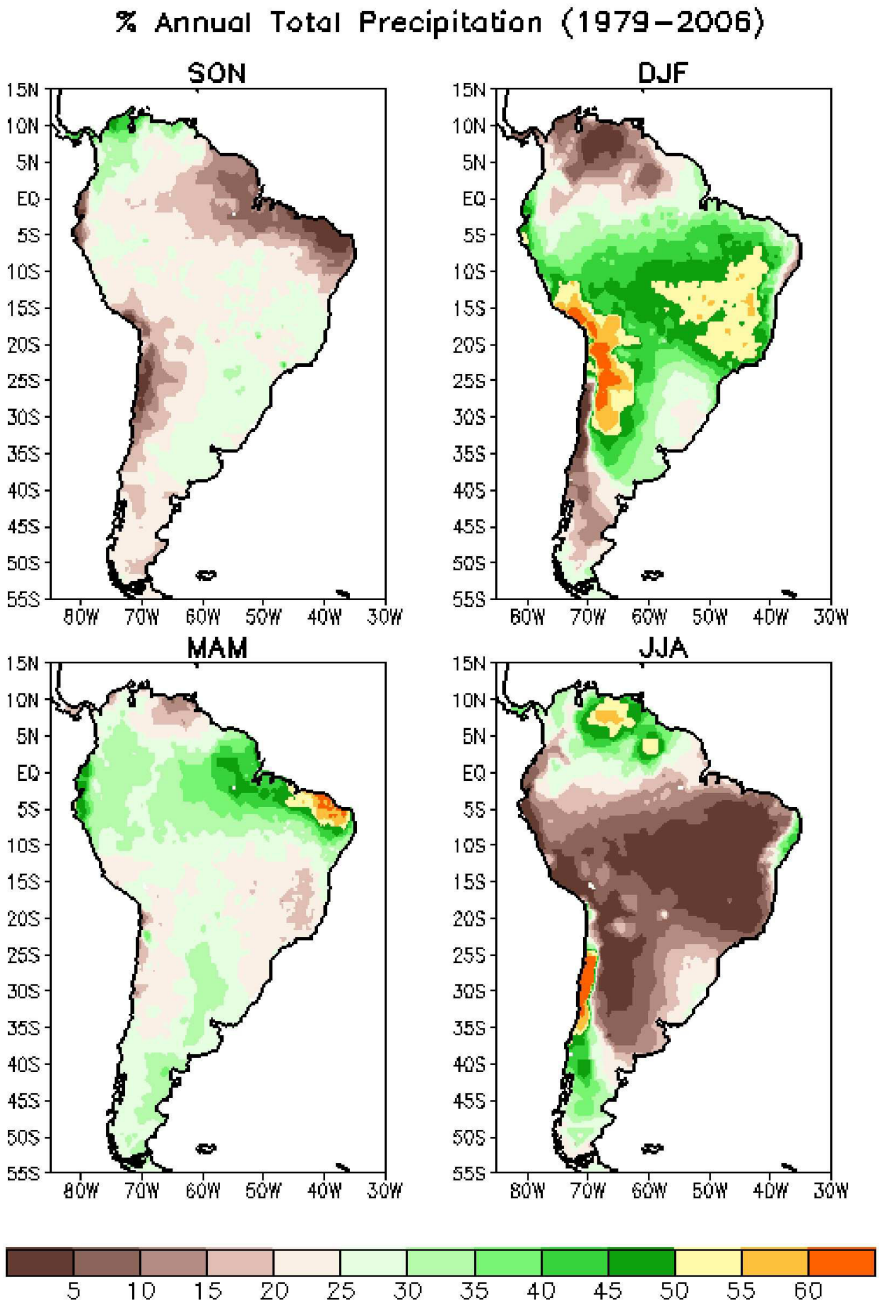

Fig. 5. Percent of observed mean (1979-2006) annual precipitation for each season.

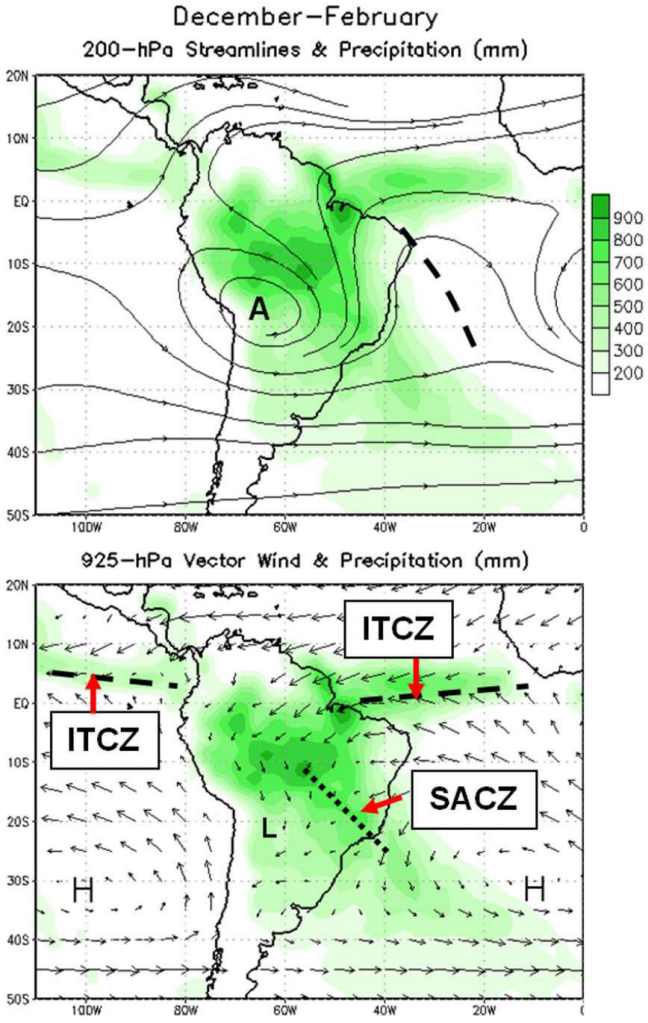

Fig. 6. Mean 200-hPa vector wind/ streamlines and estimated precipitation (mm) (top) and 925-hPa vector wind/ streamlines and estimated precipitation (bottom). The climatology period for the circulation fields is 1979-2010 and for precipitation is 1979-1995 (CAMS OPI).

The annual cycle of upper-tropospheric circulation features over South America is intimately linked to the seasonally varying horizontal temperature gradients, which arise from differential heating due to the difference in the thermal capacity between land and water. During summer, temperatures over the continent become warmer than the neighboring oceanic regions. This results in a direct thermal circulation with low-level (upper-level) convergence (divergence), mid-tropospheric rising motion and precipitation over the continent, and low-level (upper-level) divergence (convergence), mid-tropospheric sinking motion and dry conditions over the neighboring oceanic areas (Fig. 7, top left panel). These features are typical of summertime monsoons. During winter, temperatures over the continent and nearby oceanic regions are more uniform in the zonal (east-west) direction, which gives rise to a more zonally symmetric upper-tropospheric circulation pattern over the region (Fig. 7, lower right panel) and little or no evidence of any east-west direct thermal circulation (Fig. 7, top right panel).

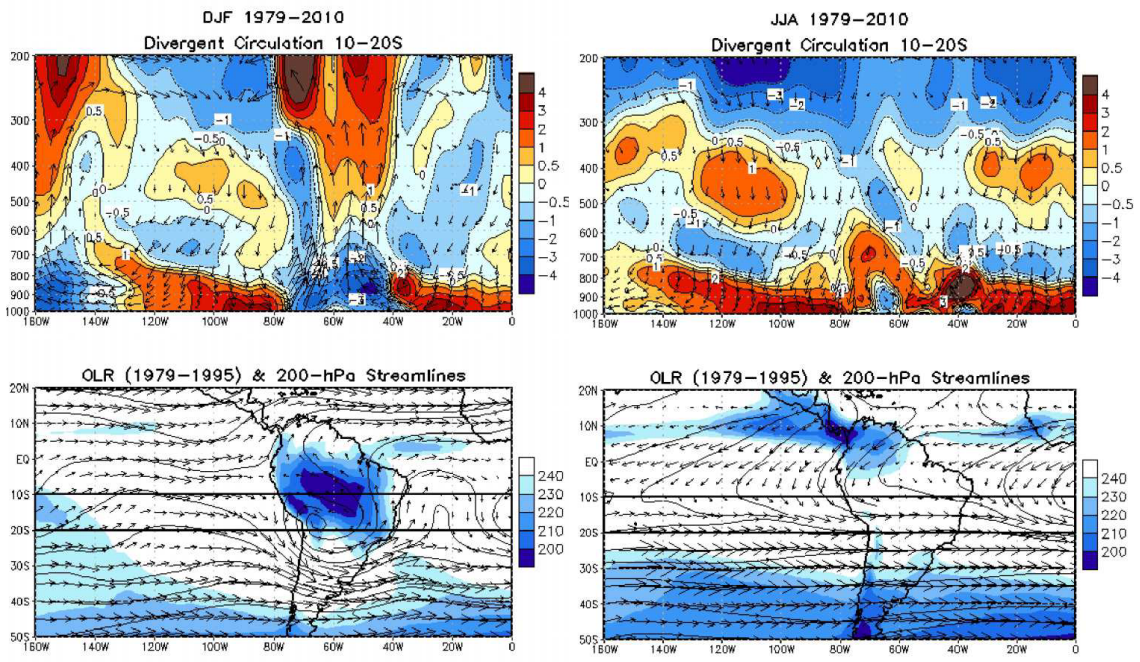

Fig. 7. Height-longitude cross-sections of the mean (1979-2010) divergent circulation (vectors) for the latitude band 10º-20ºS (top panels) and mean (1979-2010) 200-hPa vector wind, streamlines and OLR (bottom panels) for December-February (left panels) and June-August (right panels). Units are 10^{-6} s^{-1} for divergence (contours and shading in top panels) and W m^{-2} for OLR (shading in bottom panels).

3.3 Onset, mature and demise phases

The development of the South American warm season Monsoon System during the austral spring is characterized by a rapid southward shift of the region of intense convection from northwestern South America to the southern Amazon Basin and Brazilian highlands (Altiplano) (Kousky, 1988; Horel et al., 1989; Marengo et al., 2001; Liebmann & Marengo, 2001; Nogues-Paegle et al., 2002) (Fig. 8). Deep convection increases over the western Amazon Basin in September and subsequently expands southward and southeastward, reaching central Brazil in October and Southeast Brazil in November. Lower-tropospheric (850-hPa) temperatures reach their annual maximum over the southern Amazon and BP region in early September, just prior to the onset of the rains (Fig. 9).

Transient synoptic systems at higher latitudes play an important role in modulating the southward shift in convection. Cold fronts that enter northern Argentina and southern Brazil are frequently accompanied by enhanced deep convection over the western and southern Amazon and an increase in the southward flux of moisture from lower latitudes (e.g., Garreaud & Wallace, 1998). These cold fronts are also important in the formation of the South Atlantic Convergence Zone (SACZ) (e.g., Garreaud & Wallace, 1998), which becomes established in austral spring over Southeast Brazil and the neighboring western Atlantic (see Fig. 8, middle column). During spring an upper-tropospheric anticyclone (Bolivian High) becomes established near 15ºS, 65ºW (Fig. 8), as the monsoon system develops mature-phase characteristics. Upper-level troughs and dry conditions are found over oceanic areas to the

east and west of the Bolivian High. The deep convection over central Brazil and the Bolivian High reach their peak intensities during December-March. These features shift northward and weaken during April and May, as the summer monsoon weakens and a transition to drier conditions occurs over subtropical South America.

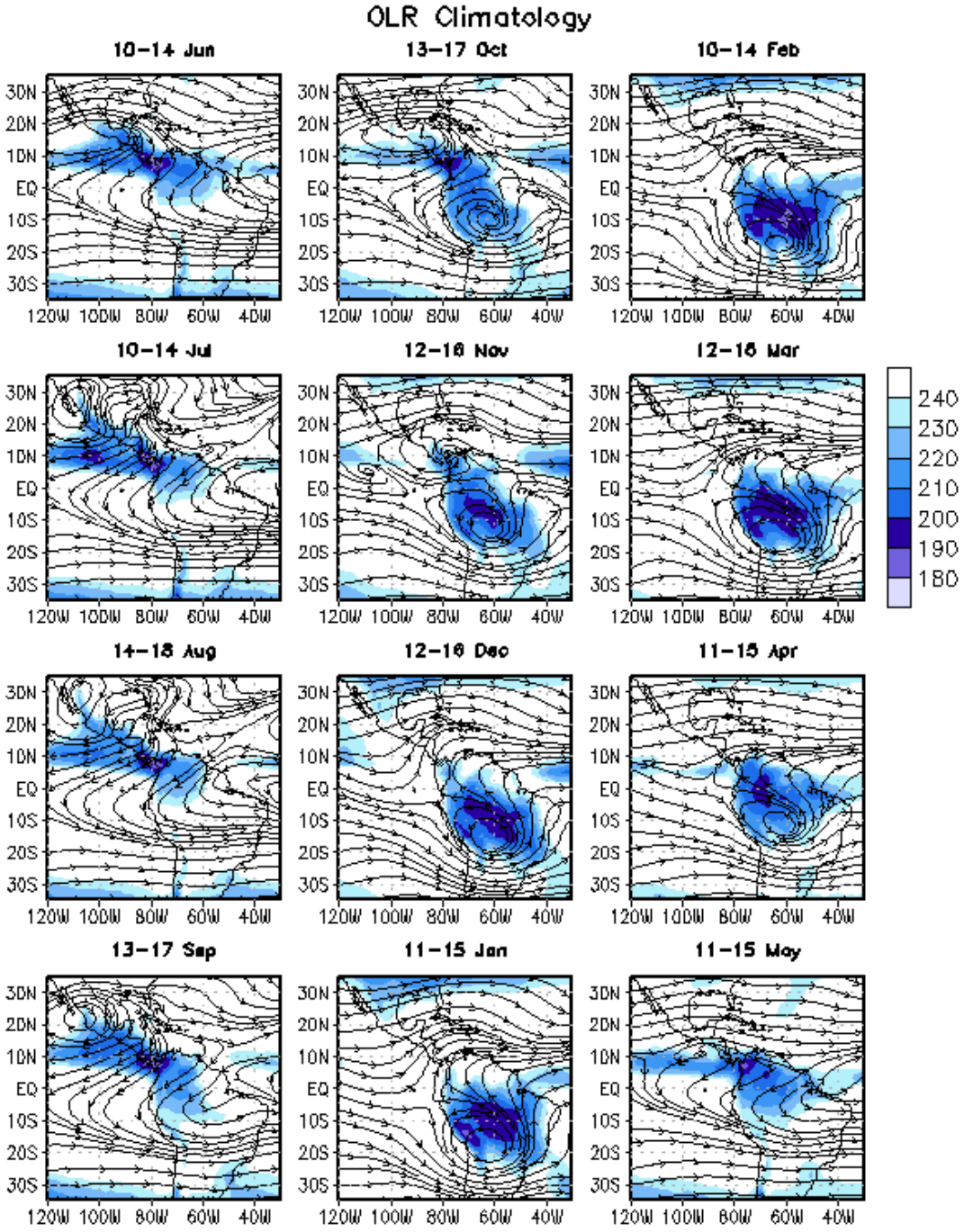

Fig. 8. Mean (1979-1995) seasonal cycle of OLR and 200-hPa streamlines. Units for OLR are W m^{-2}. Low values of OLR indicate cold cloud tops (deep convection) in the Tropics.

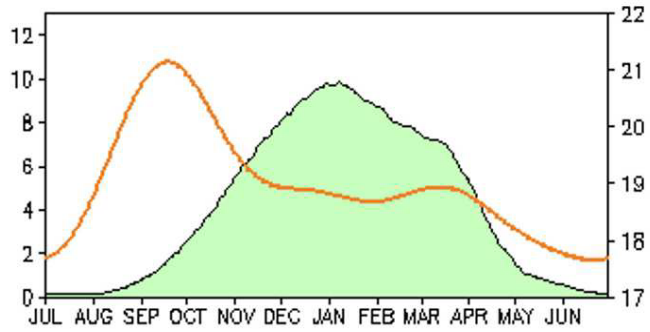

Fig. 9. Mean (1979-1995) daily precipitation (mm) for central Brazil (12.5º-17.5ºS, 47.5º-52.5ºW (shaded in green), and 850-hPa temperature (degrees C, red curve). The 850-hPa temperature data are taken from the R1 data archive.

There are many indexes in the literature that define the SAMS onset, each one with its unique characteristics (eg., Kousky, 1988; Marengo et al., 2001; Gan et al., 2006; Gonzales et al., 2007; Silva & Carvalho, 2007; Raia & Cavalcanti, 2008; Garcia & Kayano, 2009; Nieto-Ferreira & Rickenbach, 2010). The onset/end dates of the SAMS wet season, based on outgoing longwave radiation (OLR, a proxy for deep convection in the Tropics) (Kousky, 1988), are shown in Fig. 10. The wet season onset occurs in mid-September over the western Amazon basin, in mid-October over central Brazil (including the BP region), and in mid-November in Southeast Brazil. The end of the wet season occurs in early April over central Brazil, and in mid- to late May over the southern Amazon basin.

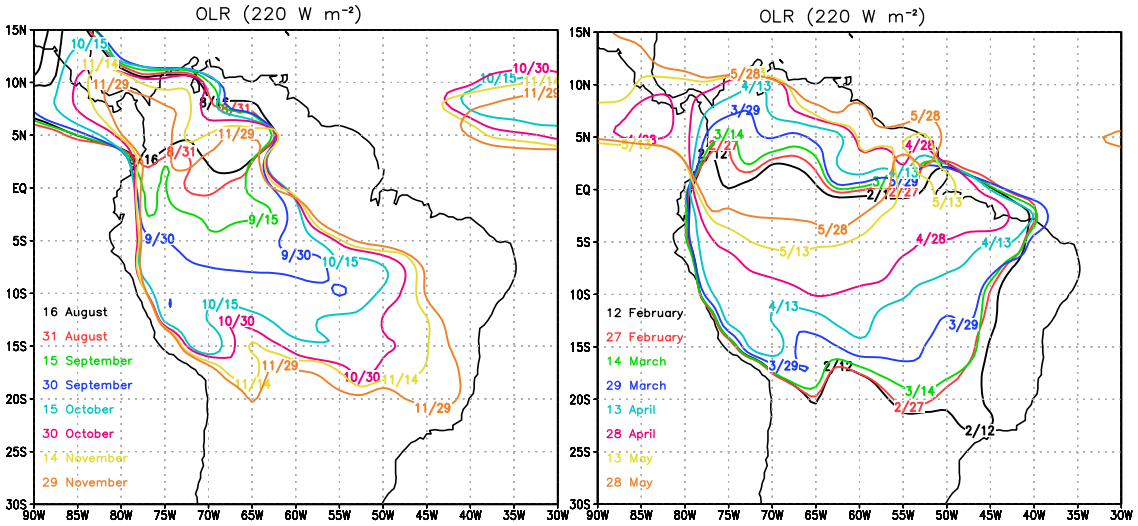

Fig. 10. Time onset and end dates for the wet season in the monsoon core region (Central Brazil) based on OLR less than 220 W m-2.

4. Variability of SAMS

4.1 Interannual variability

The phases of the EL Nino Southern Oscillation (ENSO) cycle (moderate to strong El Nino and La Nina episodes) have significant impacts on SAMS and the rainfall pattern over

tropical South America (e.g. Hastenrath & Heller, 1977; Ropelewski & Halpert, 1987; Aceituno, 1988; Kousky & Kayano, 1994; Silva et al., 2007). Mossman (1924) was one of the first to notice the relationship between the Southern Oscillation and rainfall over central South America. He showed that the Paraná River level increases during the negative (warm) phase of the Southern Oscillation (El Niño). Subsequent studies (Streten, 1983; Kousky et al., 1984; Ropelewski & Halpert, 1987, 1989; Grimm et al., 1998) demonstrated that wetter-than-average conditions occur over southeast South America during El Niño, consistent with the results of Mossman (1924).

Since the extreme phases of the ENSO cycle tend to peak during the austral summer, Silva et al. (2007) elected to use water-year (July–June) rainfall departures to show ENSO-related interannual variability over Brazil. The pattern of anomalous precipitation during El Niño episodes (Fig. 11) shows considerable event-to-event variability, especially in the magnitude of the departures. The strongest El Niño episodes (1982/83, 1991/92, and 1997/98) feature

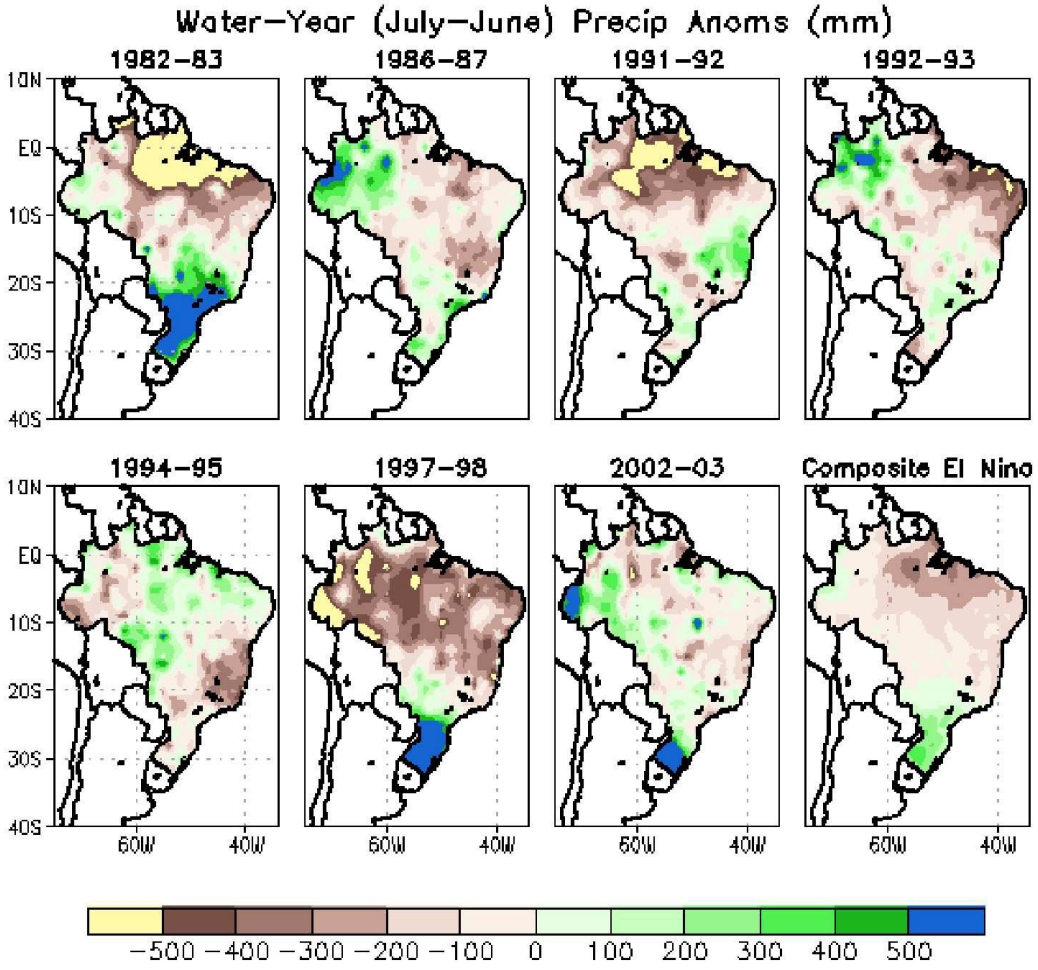

Fig. 11. Precipitation anomalies for water years (July–June) during El Niño episodes. The composite for the seven episodes is shown in the lower right-hand panel. Anomalies (mm) are computed with respect to the July 1977–June 2004 base period means. (Figure taken from Silva et al., 2007)

large precipitation deficits over the Amazon basin. The weaker events tend to have weaker precipitation anomalies. Most of the events also feature excess precipitation in southern Brazil, a region that sometimes experiences disastrous flooding related to strong El Niño episodes such as 1982/83 (Kousky et al., 1984). The composite for the seven El Niño episodes shows precipitation deficits in the central and eastern Amazon, and over northeast Brazil, and precipitation surpluses in southern Brazil, consistent with previous studies on ENSO cycle impacts (e.g., Ropelewski & Halpert, 1987, 1989; Grimm et al., 1998).

The precipitation anomaly patterns during La Niña episodes (Fig. 12) show more event-to-event consistency compared to those for El Niño. Above-average precipitation is evident over the northern part of Brazil in all six La Niña episodes. There is also a tendency for wetter-than-average conditions (four out of six cases) to occur over northeast Brazil. The composite pattern for the water-year precipitation anomalies during La Niña episodes does not reflect substantial dryness in southern Brazil, which is a feature associated with La Niña at certain times of the year (e.g., Ropelewski & Halpert, 1989; Grimm et al., 1998).

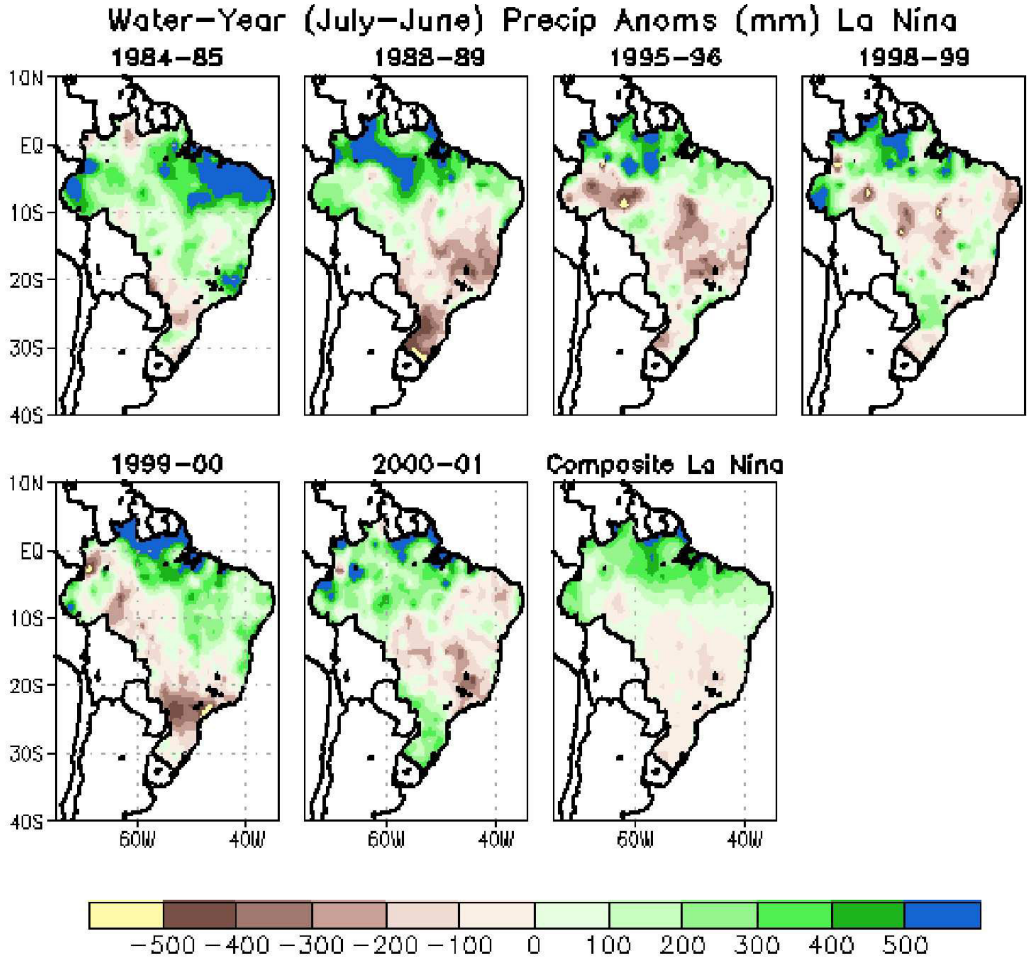

Fig. 12. Precipitation anomalies for water years (July–June) during La Niña episodes. The composite for the six episodes is shown in the lower right-hand panel. Anomalies (mm) are computed with respect to the July 1977–June 2004 base period means. (Figure taken from Silva et al., 2007)

The Atlantic SST anomaly dipole pattern (e.g., Hastenrath & Heller, 1977; Markham & McLain, 1977; Moura & Shukla, 1981; Servain, 1991; Nobre & Shukla, 1996) has a profound influence on rainfall over northeastern Brazil (the eastern flank of the SAMS). The dipole pattern usually consists of SST anomalies of one sign north of the equator and SST anomalies of the other sign south of the equator, which results in an anomalous displacement of the equatorial trough and Intertropical Convergence Zone (ITCZ). Rainfall deficits and drought over northern Northeast Brazil accompany positive SST anomalies north of the equator, negative SST anomalies south of the equator, and an anomalously northward displaced ITCZ. In contrast, above-average rainfall in northern Northeast Brazil accompanies negative SST anomalies north of the equator, positive SST anomalies south of the equator, and an anomalously southward displaced ITCZ (Fig. 13).

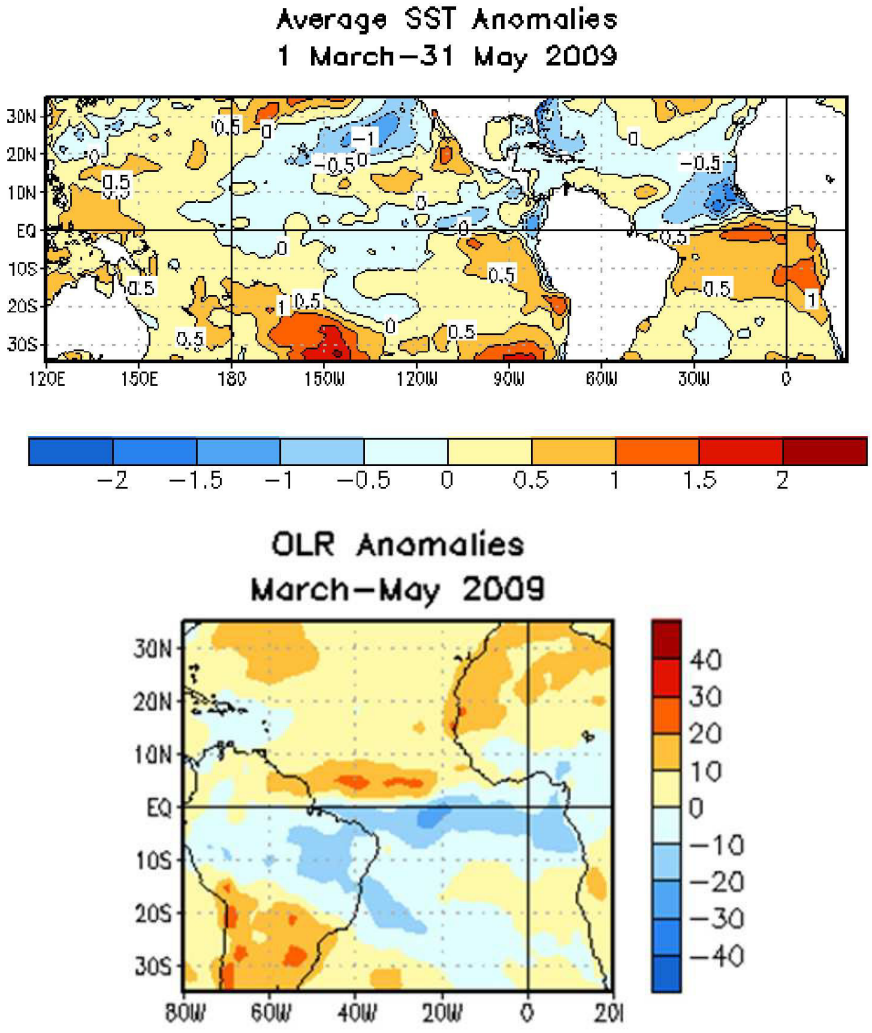

Fig. 13. Sea surface temperature anomalies (°C) (left panel) and outgoing longwave radiation anomalies (W m^{-2}) for March-May 2009 (right panel). SST anomalies are departures from the 1971-2000 base period means and OLR anomalies are departures from the 1979-1995 base period means. Negative OLR anomalies in the Tropics indicate enhanced convection and above-average rainfall.

4.2 Intraseasonal variability

4.2.1 SAMS and the Madden-Julian Oscillation (MJO)

Several studies have shown that the SAMS can be influenced by the Madden-Julian Oscillation (MJO). The MJO is a naturally occurring intraseasonal fluctuation in the global tropics, with a typical period of 30-60 days (Madden & Julian, 1971, 1972; Madden & Julian, 1994; Zhang, 2005). The MJO is a significant cause of weather variability in the Tropics and Subtropics that affects several important atmospheric and oceanic parameters, including lower- and upper-level wind speed and direction, cloudiness, rainfall, sea surface temperature (SST), and ocean surface evaporation. The enhanced rainfall phase of the MJO can affect both the timing of a monsoon onset and monsoon intensity. Moreover, the suppressed phase of the MJO can prematurely end a monsoon and initiate breaks during monsoon wet seasons.

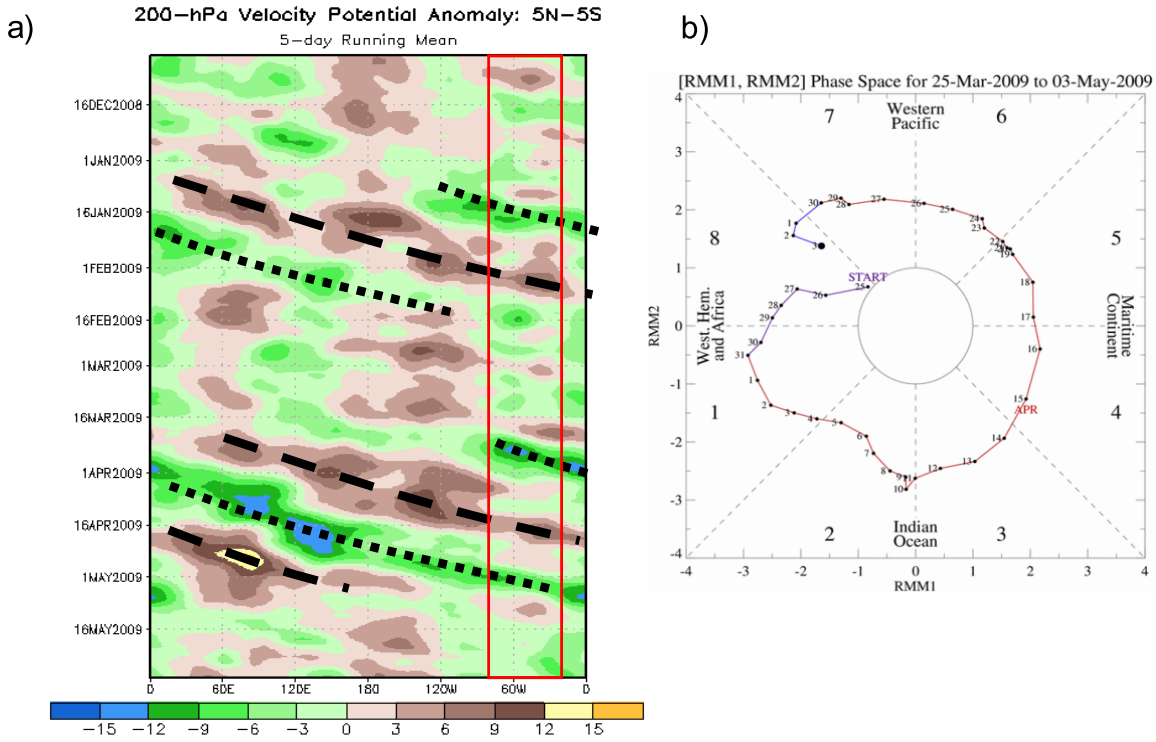

Fig. 14. a) Time longitude section of 200-hPa velocity potential anomalies in the latitude band 5ºN-5ºS, and b) the NOAA/Climate Prediction Center version of the Wheeler and Hendon (2004) daily MJO index.

The MJO modulates summer rainfall over northern and northeastern South America. It is very important for Northeast Brazil (semi-arid region), which experiences a short (3-4 months) wet season. An example of MJO-related heavy rainfall events occurred during March-May 2009. From mid-March to early May 2009, eastward propagating velocity potential anomalies (Fig. 14a) indicate moderate-to-strong MJO activity. The active phase of the MJO was in the South American sector (Fig. 14b, phase 8) during the end of March and again in the beginning of May, contributing to excessive rainfall and flooding over portions of northeastern Brazil, especially in early May (Fig. 15). Another factor contributing to the excessive seasonal rainfall

was the presence of the Atlantic SST dipole (discussed in the previous section), which favored an anomalously southward displaced ITCZ and enhanced rainfall over Northeast Brazil.

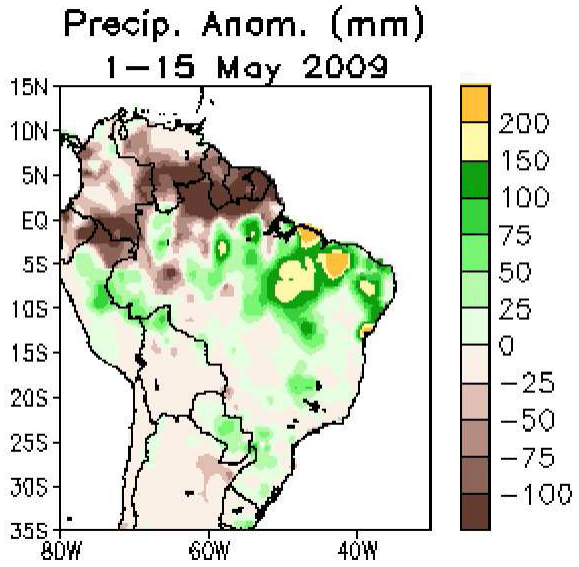

Fig. 15. Precipitation anomalies (mm) for 1-15 May 2009. Anomalies are departures from the 1979-2010 base period.

4.2.2 SAMS and the South Atlantic Convergence Zone

A characteristic feature of anomalous precipitation over South America is the tendency for a dipole pattern to occur, with anomalies of one sign located in the region of Southeast Brazil, the climatological position of the South Atlantic Convergence Zone (SACZ), and anomalies of the other sign situated over southeastern South America (southern Brazil, Uruguay, Paraguay and northeastern Argentina (e.g., Casarin & Kousky, 1986; Kousky & Cavalcanti, 1988; Kayano & Kousky, 1996; Nogues-Paegle & Mo, 1997; Herdies et al., 2002; Nogues-Paegle et al., 2002; Diaz & Aceituno, 2003; Silva & Berbery, 2005; Marengo et al., 2010). This dipole pattern has been shown to be partly related to the phasing of synoptic waves with the phase of the MJO (e.g., Casarin and Kousky, 1986; Nogues-Paegle et al., 2002; Liebmann et al., 2004; Carvalho et al., 2004; Cunningham & Cavalcanti, 2006).

Mid-latitude frontal systems (e.g., Kousky 1979, 1985; Garreaud & Wallace 1998) have an important effect on the intensity and distribution of deep convection over tropical and subtropical South America, and the location of the SACZ. As cold fronts move northward over southern Brazil, they organize a band of intense convection stretching along the front, often extending from the slopes of the Andes eastward to the western Atlantic. This band of intense convection shifts northward accompanying the advance of the front, and may eventually reach as far north as the Amazon basin and Northeast Brazil.

Subtropical upper-level cyclonic vortices (Kousky & Gan, 1981) also affect the distribution and intensity of rainfall, particularly over eastern Brazil. These systems typically form within the Atlantic mid-oceanic trough, near the coast of Northeast Brazil. Once formed they tend to drift slowly westward with time, often moving over Northeast Brazil. These vortices are cold core systems characterized by a central region of relatively dry sinking air, while on

the western, northern, and sometimes eastern flanks of these systems convection is often enhanced, resulting in heavy rainfall.

4.3 SAMS diurnal variability

Major features of the summertime diurnal cycle for the South American region, as depicted in the NOAA/Climate Prediction Center Morphing technique (CMORPH) precipitation analyses (Joyce et al. 2004), include an afternoon (18-21 UTC) maximum in precipitation over the Andes and the high terrain in central and eastern Brazil, a nocturnal (06-09 UTC) maximum in precipitation over areas just east of the Andes (over western Argentina, central Bolivia, and western Paraguay), and an early morning (12-15 UTC) maximum over the Atlantic Ocean in the vicinity of the South Atlantic Convergence Zone (Fig. 16, and as described in

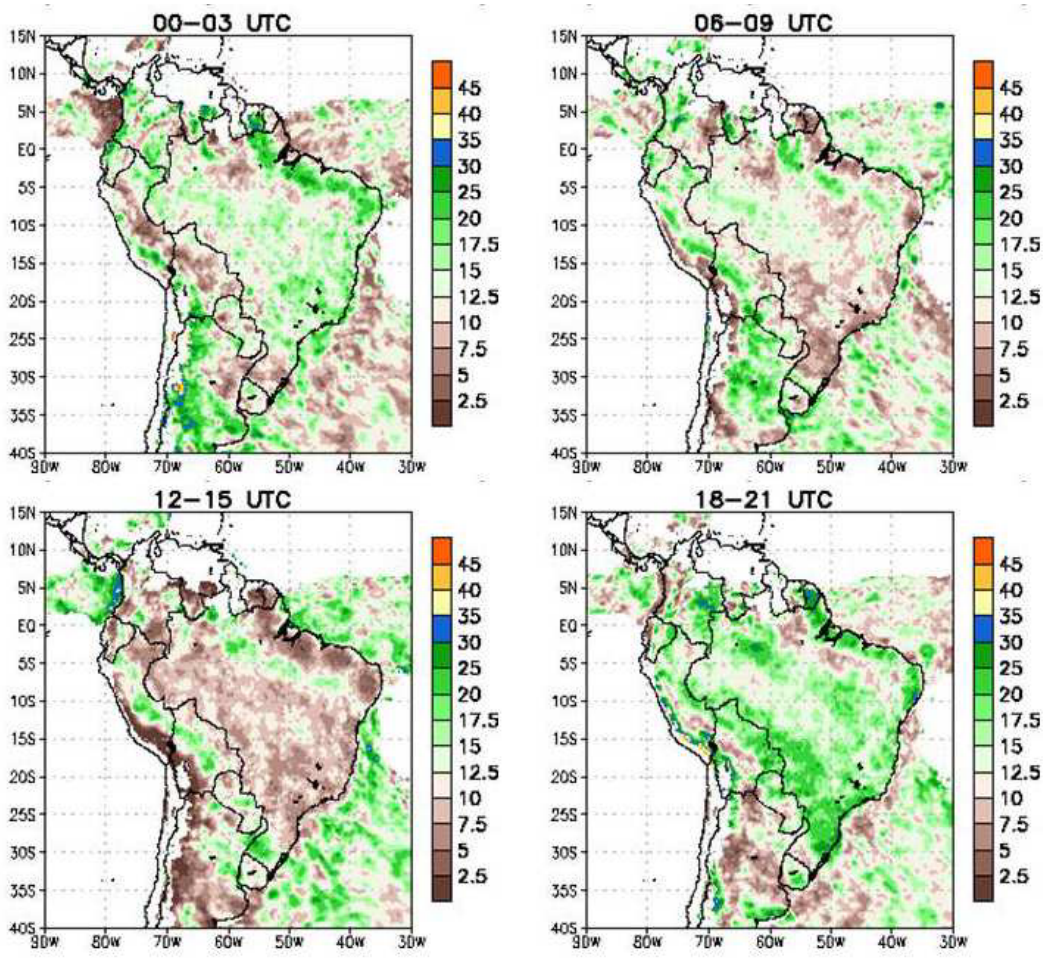

Fig. 16. Mean percentage of daily total precipitation for 00-03 UTC (20-23 LST), 06-09 UTC (02–05 LST), 12-15 UTC (08–11 LST), and 18-21 UTC (14-17 LST). Local standard time (LST) is for the center longitude of the domain. The mean is computed for the combined December–February periods for 2002–2003 and 2003–2004. Note: if rainfall were distributed equally throughout the 24-hour period, then 12.5% would be the expected percentage of the daily total for each 3-hour interval. Percentages have been masked out in regions where rainfall average is less than 1 mm day^{-1}.

Janowiak et al. 2005). A nocturnal or early morning (12-15 UTC) precipitation maximum also occurs along the immediate coast and offshore in the vicinity of the Atlantic ITCZ and over the Pacific near the coast of Colombia, consistent with the hypothesis presented by Silva Dias et al. (1987) that an out-of-phase relationship exists in the diurnal cycles of continental and nearby oceanic regions.

A remarkable diurnal cycle in precipitation occurs in coastal areas of northern and northeastern South America. With daytime heating, precipitation rapidly develops along and just inland from the coast (Fig. 16, lower right panel), probably related to the sea breeze (Kousky, 1980; Garstang et al., 1994; Negri et al,. 2002). This precipitation advances westward and southward with time, producing a nocturnal maximum in areas approximately 500 km inland from the coast (Fig. 16, upper right panel). The average diurnal cycle for equatorial South America (equator to 5°N) for March–May 2003–2004 (Fig. 17) indicates that sea-breeze-induced precipitation systems propagate westward (dashed lines), reaching the western Amazon Basin in about two days. As these systems propagate inland, they contribute to a nocturnal precipitation maximum in some areas and a diurnal precipitation maximum in other areas. The nocturnal maximum in precipitation over the central Amazon basin and the inland propagation of sea-breeze-induced rainfall systems are most often observed during January-May (Fig. 18), when the diurnal cycle in the central Amazon basin displays two maxima (one nocturnal and the other diurnal). Propagating features can also be found east of the Andes Mountains over northern Argentina. Daytime heating initiates convection along the east slopes of the Andes, which subsequently propagates eastward over the low lands of northern Argentina and Paraguay resulting in a nocturnal maximum in those regions. Similar propagating features have been observed over the central Plains east of the Rocky mountains of the United States (e.g., Carbone et al. 2002; Janowiak et al. 2005).

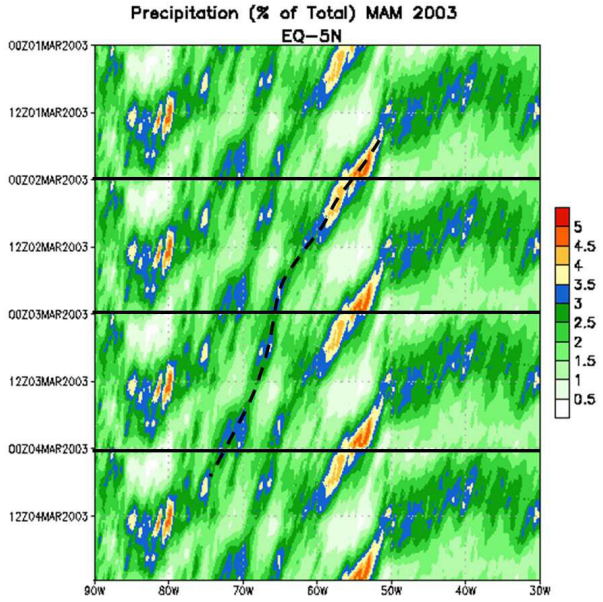

Fig. 17. Time-longitude section of the mean (March-May 2003) percentage of daily precipitation for the latitude band 0º-5ºN. The mean diurnal cycle is repeated 4 times. The dashed line indicates the westward propagation with time associated with sea-breeze-induced convection along the northeast coast of South America (vertical dashed line near 50ºW).

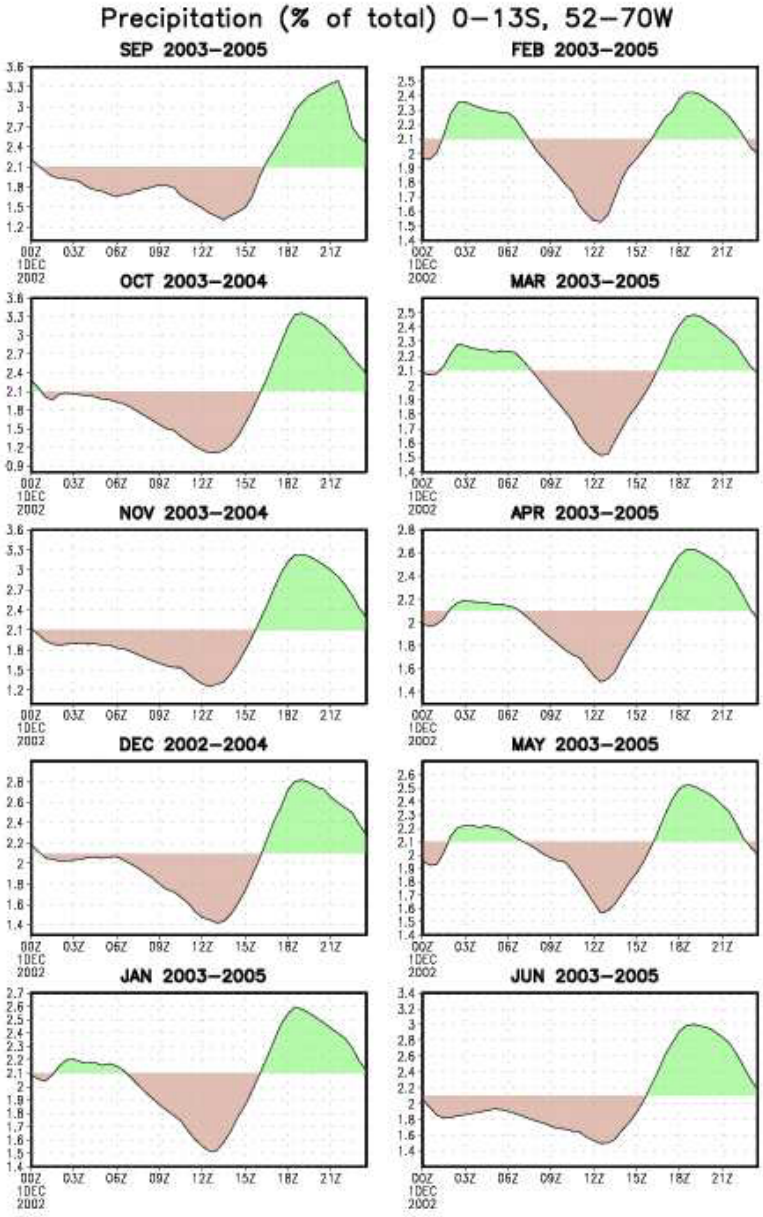

Fig. 18. The annual cycle of the mean diurnal cycle for the central Amazon basin (0º-13ºS, 52º-70ºW. Local time is approximately 4 hours less than UTC (Z).

4.4 Extreme precipitation events

As mentioned in the introduction, heavy rainfall events near Brazil's heavily populated east coast can result in disastrous flooding, with loss of life, property and infrastructure. A climatology of intense rainfall events is presented for three regions in eastern Brazil shown in Fig. 19. The daily average precipitation in each of the 5x5 degree boxes was computed during the 32-year period 1979-2010. Next the daily data were stratified by month and the number of cases for precipitation equal to or exceeding selected thresholds

(10, 15, 20, 25, 30, 35, 40, 45, and 50 mm) was computed. The results are shown in Tables 1-3. The greatest number of cases among the three regions and for all thresholds occurs in region-3 (Southeast Brazil, Table 1) during the height of the SAMS wet season (December-January). A similar peak, but with fewer cases is observed in region-2 (Table 2), which also has a secondary peak in March. Region-1 (Table 3) has fewer cases than in the other two regions for all thresholds, and, as in region-2, features two peaks (January and March) for thresholds below 20 mm.

The daily values for each month were ranked (highest to lowest) and the top 20 cases for each region (Table 4) were selected for further analysis. To determine the independent events in each region, cases where the dates are close together (within 5 days) are considered as a single event. Thus, the number of events in the top 20 cases (Table 4) is 14 for region-3, 12 for region-2 and 7 for region-1. This indicates a tendency for extreme events to persist for longer periods of time at lower latitudes over eastern South America.

The sea level pressure (SLP) and precipitable water (PW) analyses for the top 12 events in region-3 (indicated by the red asterisks in Table 1) are shown in Fig. 20. All of the events show high values of PW and a SLP trough in the vicinity of Southeast Brazil. In most cases, high PW values and a pressure trough extend in a band eastward/southeastward over the Atlantic Ocean. Since PW depends primarily on moisture available in the lowest layers of the atmosphere, bands of high PW are usually co-located with regions of low-level convergence, which accompany surface cold fronts or remnant pressure troughs. Of the 12 events shown in Fig. 20, only two events (17 January 1980 and 9 January 2004) do not show any apparent relationship with fronts.

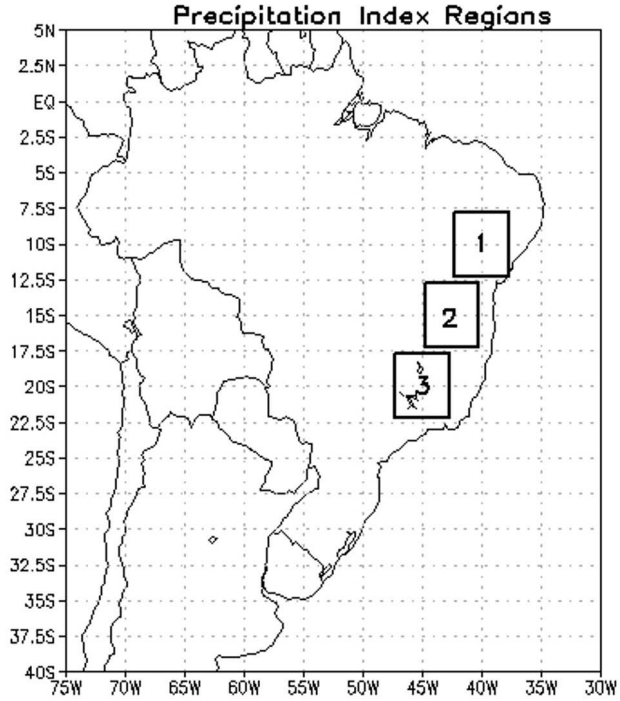

Fig. 19. Precipitation Index for selected regions.

Region-3 (17.75-22.25S, 42.75, 47.25W)									
	≥10mm	≥15mm	≥20mm	≥25mm	≥30mm	≥35mm	≥40mm	≥45mm	≥50mm
JUL	8	3	0	0	0	0	0	0	0
AUG	6	1	1	1	0	0	0	0	0
SEP	35	17	5	1	0	0	0	0	0
OCT	87	35	12	3	1	0	0	0	0
NOV	229	99	37	10	3	3	3	0	0
DEC	349	182	77	35	16	4	2	1	0
JAN	366	190	79	40	14	7	4	3	1
FEB	207	100	36	14	4	3	2	0	0
MAR	178	71	31	6	1	0	0	0	0
APR	43	19	5	3	1	0	0	0	0
MAY	21	11	7	3	2	0	0	0	0
JUN	6	4	3	1	0	0	0	0	0

Table 1. Number of events P ≥ given thresholds for Region-3.

Region-2 (12.75-17.25S, 40.25, 44.75W)									
	≥10mm	≥15mm	≥20mm	≥25mm	≥30mm	≥35mm	≥40mm	≥45mm	≥50mm
JUL	0	0	0	0	0	0	0	0	0
AUG	0	0	0	0	0	0	0	0	0
SEP	5	1	1	0	0	0	0	0	0
OCT	40	18	7	4	0	0	0	0	0
NOV	153	62	24	11	5	2	0	0	0
DEC	204	97	41	13	4	2	1	0	0
JAN	162	84	36	12	3	2	0	0	0
FEB	81	42	21	6	3	2	0	0	0
MAR	113	50	16	7	0	0	0	0	0
APR	23	6	0	0	0	0	0	0	0
MAY	0	0	0	0	0	0	0	0	0
JUN	1	1	0	0	0	0	0	0	0

Table 2. Number of events P ≥ given thresholds for Region-2.

Region-1 (7.75-12.25S, 37.75, 42.25W)									
	≥10mm	≥15mm	≥20mm	≥25mm	≥30mm	≥35mm	≥40mm	≥45mm	≥50mm
JUL	0	0	0	0	0	0	0	0	0
AUG	0	0	0	0	0	0	0	0	0
SEP	2	0	0	0	0	0	0	0	0
OCT	11	1	1	0	0	0	0	0	0
NOV	30	11	5	1	0	0	0	0	0
DEC	58	22	7	2	1	0	0	0	0
JAN	67	34	15	7	2	2	0	0	0
FEB	60	25	7	4	1	0	0	0	0
MAR	87	26	11	2	0	0	0	0	0
APR	40	12	4	1	1	0	0	0	0
MAY	6	3	1	0	0	0	0	0	0
JUN	2	0	0	0	0	0	0	0	0

Table 3. Number of events P ≥ given thresholds for Region-1.

	Region-3	Precipitation (mm)	Region-2	Precipitation (mm)	Region-1	Precipitation (mm)
1	3-Jan-97*	52.3	30-Jan-92	38.8	14-Jan-04	38.8
2	3-Jan-00*	47.3	17-Jan-04	35.1	28-Jan-92	36.2
3	4-Jan-97	45.7	16-Jan-02	31.9	20-Jan-04	28.2
4	23-Jan-92*	41.4	13-Jan-92	28.9	17-Jan-04	28.0
5	24-Jan-92	39.2	9-Jan-79	28.6	3-Jan-02	26.8
6	2-Jan-00	37.2	10-Jan-79	28.2	30-Jan-92	26.1
7	9-Jan-85*	35.8	5-Jan-09	26.7	29-Jan-92	25.5
8	3-Jan-82*	34.5	15-Jan-80	26.6	18-Jan-04	22.9
9	6-Jan-83*	34.0	28-Jan-92	26.3	24-Jan-04	22.6
10	25-Jan-85*	33.3	15-Jan-02	26.3	11-Jan-99	22.6
11	26-Jan-85	32.3	17-Jan-79	25.4	18-Jan-02	22.5
12	6-Jan-97	31.8	14-Jan-80	25.1	15-Jan-79	21.9
13	12-Jan-81*	30.2	2-Jan-02	24.7	19-Jan-04	20.7
14	30-Jan-08*	30.1	11-Jan-85	24.2	17-Jan-79	20.6
15	17-Jan-80*	29.9	1-Jan-83	24.1	21-Jan-00	20.4
16	9-Jan-04*	29.4	8-Jan-79	24.1	5-Jan-02	19.9
17	24-Jan-82*	29.3	1-Jan-81	23.7	7-Jan-02	19.7
18	12-Jan-91	29.1	27-Jan-92	23.7	26-Jan-92	19.3
19	16-Jan-91	29.0	25-Jan-92	23.6	21-Jan-04	19.2
20	28-Jan-91	28.8	6-Jan-09	23.4	8-Jan-02	19.0

Table 4. Top 20 precipitation cases during January (1979-2010) for the three regions in Fig. 19. The red asterisks indicate the 12 events used in Fig. 20.

The austral summer 1999-2000 featured considerable intraseasonal variability in the intensity and location of convection over eastern Brazil (Silva & Kousky, 2001). The lowest values of OLR (strongest deep convection) during the period were observed over Southeast Brazil during 1-5 January 2000 (3 January 2000 is ranked number two for the extreme events in region-3, Table 4). During this period, precipitation exceeded 150 mm (Fig. 21, left panel) over a large portion of Southeast Brazil, resulting in mudslides, flooding and loss of life. The average OLR for this period (Fig. 21, right panel) shows a well-defined band of low OLR (intense convection) extending from the Amazon basin southeastward over Southeast Brazil and the neighboring western Atlantic. The corresponding average vertical motion for this period (Fig. 22, left panel) shows that rising motion (negative omega) accompanied the band of low OLR. The average upper-tropospheric (200-hPa) wind (Fig. 22, right panel) shows a trough over costal sections of southern and southeastern Brazil, and a well-defined subtropical jet stream located near 25ºS. This jet stream has a maximum over the western Atlantic, and its left rear entrance region is located near the bands of heavy rainfall, rising motion and low OLR over Southeast Brazil. The rising motion, associated with the low OLR is accompanied by sinking motion farther southwest over southern Brazil and Paraguay (Fig. 22, left panel). These features are consistent with the typical dipole pattern in precipitation, discussed in section 4.2.2, and an intense SACZ near its climatological position over Southeast Brazil.

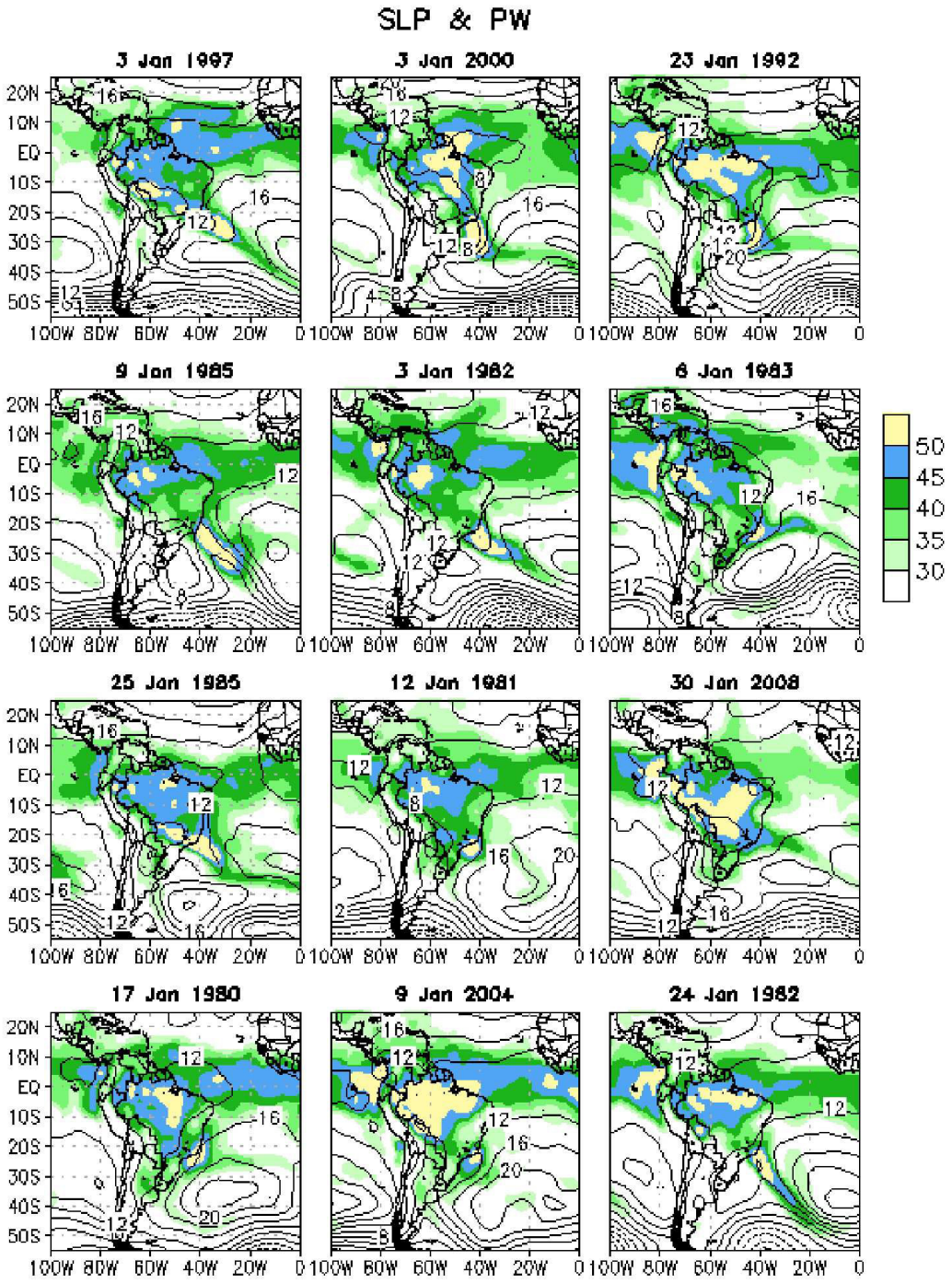

Fig. 20. Sea level pressure (contours, hPa-1000) and precipitable water (shading, mm) for 12 extreme events in region-3 (see Table 4).

The circulation features for active convection over southeastern Brazil indicate a strong coupling between the bands of enhanced convection/rising motion and the left rear

entrance region of an upper-tropospheric jet stream (Silva & Kousky, 2001; Carvalho et al., 2002). Once established, these patterns tend to persist for several days. The possible evolution leading to persistence is as follows: 1) the synoptic-scale pattern provides a mechanism (surface front and upper-level trough) to enhance convection over the high terrain regions of eastern Brazil; 2) this convection is strongly modulated by the diurnal cycle and the topography of the region; 3) local thermal contrasts, due to the distribution of clouds and precipitation, tend to favor a persistence of convection within the region; 4)

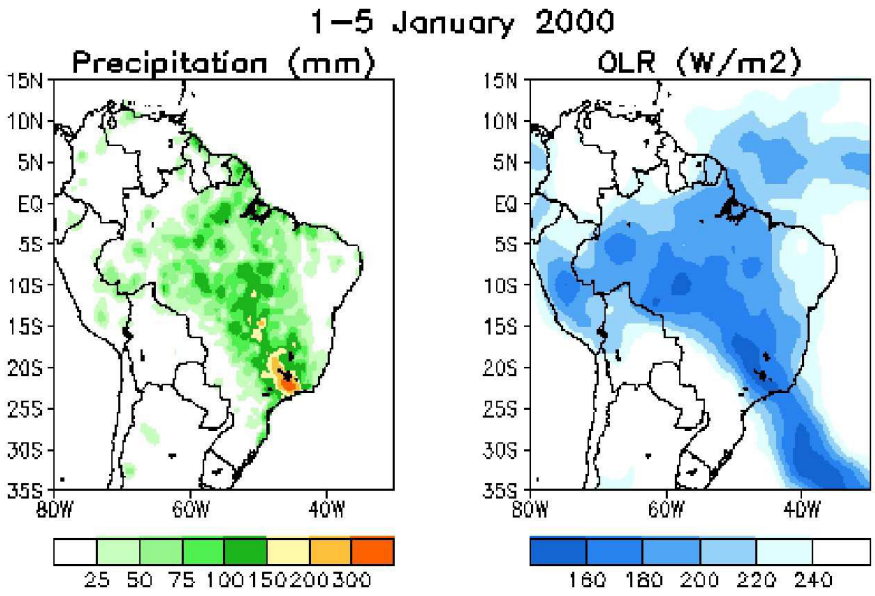

Fig. 21. Total precipitation (mm) (left panel) and average outgoing longwave radiation (OLR, W m^{-2}) (right panel) for the period 1-5 January 2000.

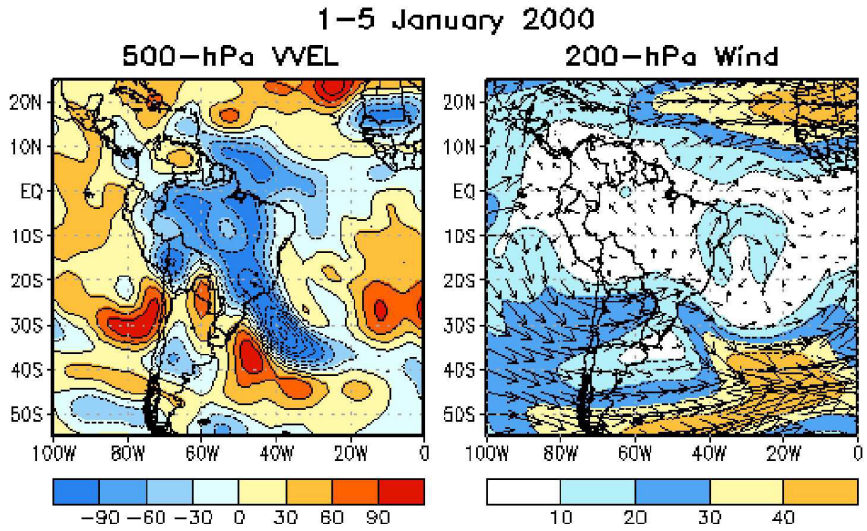

Fig. 22. Average vertical motion (omega, hPa d^{-1}) (left panel) and 200-hPa vector wind (m s^{-1}) (right panel) for the period 1-5 January 2000.

thus, anomalous latent heating in the middle and upper troposphere continues in the same area; and 5) this tends to maintain the upper-level jet stream and related low-level circulation features, such as a surface pressure trough and baroclinic zone, in approximately the same position for several days.

During December 2000-February 2001 (the peak of the wet season), large rainfall deficits (up to 400 mm, Fig. 23, right panel) were observed over Southeast Brazil (region-3 in Fig. 19) and the BP region (see Fig. 1), which are important regions for water storage and hydroelectric energy generation. As a result, Brazil experienced a major energy crisis in 2001 that led to the implementation of restrictions on energy usage throughout the country in order to avoid large-scale blackouts. Three major factors contributed to the energy crisis: 1) large rainfall deficits (Fig. 23), during the peak of the SAMS wet season, in the upper portions of the Tocantins, São Francisco and La Plata/Paraná river basins (BP region in Fig. 1, and Southeast Brazil region-3 in Fig. 19), 2) increasing energy demands, and 3) delays in implementing new power plants (Kelman et al., 2001).

The dry conditions during December 2000-February 2001 are remarkable when compared to the previous year (December 1999-February 2000, Fig. 23, left panel), which featured near- or above-average conditions over Southeast Brazil. The mean daily rainfall rate during DJF 2000-2001 was only about half the rate observed during DJF 1999-2000 (Fig. 24). The differences between the two wet seasons cannot be attributed to the ENSO cycle, since both years featured La Niña conditions in the tropical Pacific. Further investigation is necessary to identify the causes for the exceptionally dry conditions over the BP region and Southeast Brazil during the 2000-2001 wet season.

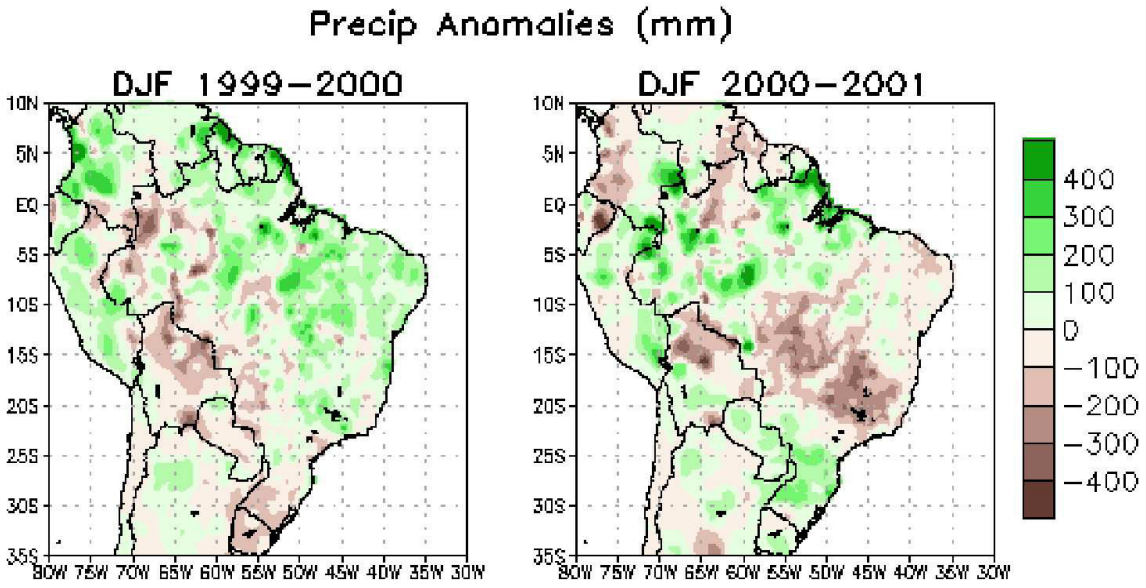

Fig. 23. Anomalous precipitation for December 1999-February 2000 (left panel) and December 2000-February 2001 (right panel). Data are derived from the daily gridded analyses of precipitation produced by the NOAA/ Climate Prediction Center. Anomalies are departures from the 1979-2010 base period mean.

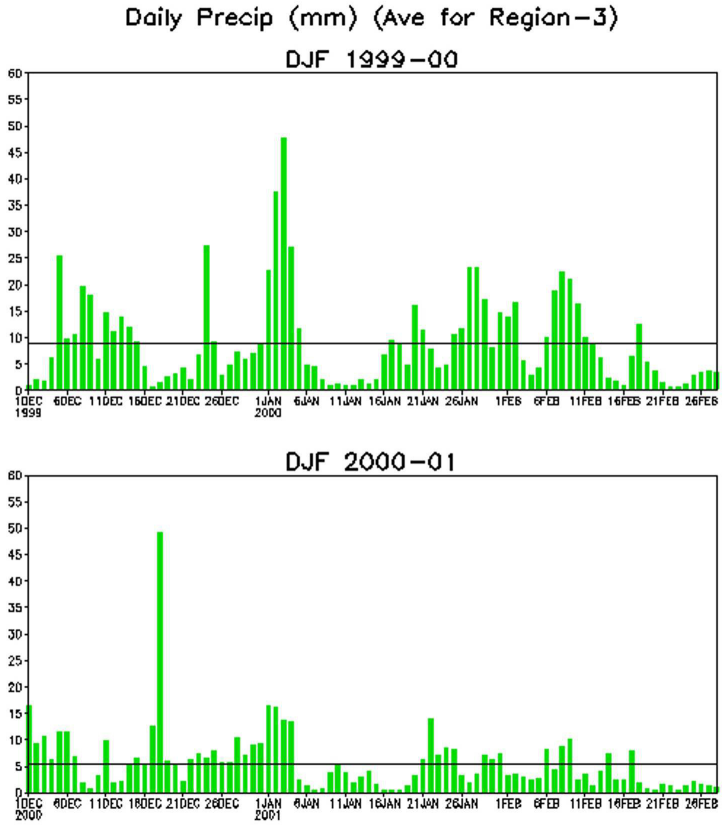

Fig. 24. Time series of daily rainfall (mm), averaged over region-3 (Fig. 19), for December 1999-February 2000 (left panel) and December 2000-February 2001 (right panel).

5. Conclusion

This chapter highlights some of the results presented in previous reviews and studies on the South American Monsoon System (SAMS), regarding circulation features, the evolution of the wet season and variability on time scales ranging from diurnal to inter-annual. In addition, a brief inter-comparison among several re-analyses during December-February indicates uncertainties in the low-level circulation features and related derived quantities, such as moisture flux, convergence and vertical motion within the core region of SAMS. These uncertainties are undoubtedly related to differences in the December-February precipitation patterns between the re-analyses and observations, which display large biases over many areas in South America. It is extremely important that future re-analyses emphasize bias reduction, in order to reduce these uncertainties.

Examples of extreme events on a variety of time scales illustrate the large range of variability associated with the SAMS wet season. Although much progress has been made in understanding the phenomena responsible for those events, further research is necessary to document their dynamical and thermodynamical causes, frequency of occurrence and predictability. Benchmark studies of this type are extremely important for decision makers as they develop plans to mitigate present and future impacts of weather and climate variability on society.

6. References

Aceituno, P. (1988). On the functioning of the Southern Oscillation in the South American sector. Part I: Surface climate. *Mon. Wea. Rev.,* Vol. 116, pp. 505–524.

Carbone, R. E.; Tuttle, J. D.; Ahijevych, D. A. & Trier, S. B. 2002. Inferences of predictability associated with warm season precipitation episodes. *J. Atmos. Sci*., Vol. 59, pp. 2033-2056.

Carvalho, L. M. V.; Jones, C. & Liebmann, B. (2002). Extreme precipitation events in Southeastern South America and large-scale convective patterns in the South Atlantic Convergence Zone. *J. Climate*, Vol. 15, pp. 2377-2394.

Casarin, D. P. & Kousky, V. E. (1986). Precipitation anomalies in Southern Brazil and related changes in the atmospheric circulation. *Revista Brasileira de Meteorologia*, Vol. 1, pp. 83-90.

Chen, M.; Shi, W., Xie, P., Silva, V. B. S., Kousky, V E., Higgins, R. W. & Janowiak, J. E. (2008). Assessing objective techniques for gauge-based analyses of global daily precipitation, *J. Geophys. Res*., Vol. 113, D04110, doi:10.1029/2007JD009132.

Cunningham, C. C. & Cavalcanti, I. F. A. (2006). Intraseasonal modes of variability affecting the South Atlantic Convergence Zone. *Int. J. Climatol*., Vol. 26, pp. 1165-1180.

Diaz, A. & Aceituno, P. 2003: Atmospheric Circulation Anomalies during Episodes of Enhanced and Reduced Convective Cloudiness over Uruguay. *J. Climate*, Vol. 16, 3171-3185.

Gan M. A.; Rodrigues L. R., Rao V. B. (2009). Monção na America do Sul. Chapter 19 in *Tiempo y Clima no Brasil*, Cavalcanti I, Ferreira N.J., Justi M. A. G. , Silva Dias M. A. F., (eds) Editora. Oficina de Textos, S˜ao Paulo: Brazil, pp. 297–312.

Gan, M. A.; Rao, V. B. & Moscati, M. C. L. (2006). South American monsoon indices. *Atmospheric Science Letters,* Vol. 6, pp. 219–223.

Gan, M. A.; Kousky, V. E. & Ropelewski, C. F. (2004). The South American Monsoon circulation and its relationship to rainfall over west-central Brazil. *J. Climate*, Vol. 17, pp. 47-66.

Garreaud, R. D. & Wallace, J. M. (1998). Summertime incursions of midlatitude air into subtropical and tropical South America. *Mon. Wea. Rev*., Vol. 126, pp. 2713-2733.

Garstang, M.; Massey Jr., H. L.; Halverson, J.; Greco, S. & Scala, J. (1994). Amazon coastal squall lines. Part I: Structure and kinematics. *Mon. Wea. Rev*., Vol. 122, pp. 608-622.

Gill, A. E. 1980. Some simple solutions for heat induced tropical circulation. *Quart. J. Roy. Meteor. Soc*., Vol. 106, pp. 447-462.

Gonzalez, M.; Vera, C., Liebmann B., Marengo, J., Kousky, V. E. & Allured, D. (2007). The nature of the rainfall onset over central South America. *Atmosfera,* Vol. 20, pp. 379–396.

Grimm, A. M.; Ferraz, S. E. T. & Gomes J. (1998). Precipitation Anomalies in Southern Brazil Associated with El Niño and La Niña Events. *J. Climate*, Vol. 11, pp. 2863–2880.

Grimm A. M.; Vera C., Mechoso R. (2005). The South American Monsoon System, Chang C-P, Wang B, Lau NC-G, (eds) The Global Monsoon System: Research and Forecast, WMO/TD 1266 – *TMRP*: pp. 542. Available at http://www.wmo.int/pages/prog/arep/tmrp/documents/globalmonsoonsystemIWM3.pdf.

Hastenrath, S. & Heller, L. (1977). Dynamics of climatic hazards in northeastern Brazil. *Quart. J. Roy. Meteor. Soc.*, Vol. 110, pp. 77-92.

Herdies, D. L.; da Silva A., Silva Dias, M. A. F. & Nieto Ferreira, R. (2002). Moisture budget of the bimodal pattern of the summer circulation over South America. *J. Geophys. Res.*, Vol. 107 (D17), 10.1029/2001JD000997.

Horel, J. D.; Hahmann, A. & Geisler, J. (1989). An investigation of the annual cycle of convective activity over the tropical Americas. *J. Climate*, Vol. 2, pp. 1388-1403.

Janowiak, J. E.; Kousky, V. E. & Joyce, R. J. (2005). Diurnal cycle of precipitation determined from the CMORPH high spatial and temporal global precipitation analyses. J. Geophys. Res., Vol. 110, D23105, doi:10.1029/2005JD006156.

Joyce, R. J.; Janowiak, J. E.; Arkin, P. A. & Xie, P. (2004). CMORPH: A method that produces global precipitation estimates from passive microwave and infrared data at high spatial and temporal resolution. *J. Hydrometeorol.*, Vol. 5, pp. 487-503.

Kalnay, E., and Coauthors (1996) The NCEP/NCAR 40-year reanalysis project. *Bull. Amer. Met Soc.,* Vol. 77, pp. 437-471.

Kanamitsu, M.; Ebisuzaki, W., Woolen, J., Yang, S. K., Hnilo, J. J., Fiorino, M. & Potter, G. L. (2002). NCEP-DOE AMIP-II reanalysis (R-2). *Bull. Amer. Met. Soc.*, Vol. 83, pp. 1631-1643.

Kayano, M. T. & Kousky, V. E. (1996). Tropical circulation variability with emphasis on interannual and intraseasonal time scales. *Rev. Bras. Meteor.*, Vol. 11, pp. 6-17.

Kelman, J.; Venture, A., Bajay, S. V., Penna, J. C., and Haddad, C. L. S. (2001). Relatório da Comissão de Análise do Sistema Hidrotérmico de Energia Elétrica: O desequilíbrio entre oferta e demanda de energia elétrica.: *Agência Nacional de Águas/ANA*. Brasília 21 July 2001.

Kousky, V. E. (1979). Frontal Influences on Northeast Brazil. *Mon. Wea. Rev.*, Vol. 107, pp. 1140-1153.

Kousky, V. E. (1980). Diurnal rainfall variation in Northeast Brazil. *Mon. Wea. Rev.*, Vol. 108, pp. 488-498.

Kousky, V. E. & Gan, M. A. (1981). Upper Tropospheric Cyclonic Vortices in the Tropical South Atlantic. *Tellus*, Vol.33, pp. 538-551.

Kousky, V. E.; Kayano, M.T., & Cavalcanti, I. F. A. (1984). A review of the Southern Oscillation: oceanic-atmospheric circulation changes and related rainfall anomalies. *Tellus*, Vol. 36A, pp. 490-504.

Kousky, V. E. (1985). Atmospheric circulation changes associated with rainfall anomalies over tropical Brazil. Mon. *Wea. Rev., Vol*. 113, pp. 1951-1957.

Kousky, V. E. (1988). Pentad outgoing longwave radiation climatology for the South America sector. *Revista Brasilera de Meteorologıa,* Vol. 3, pp. 217–231.

Kousky, V. E. & Cavalcanti, I. F. A. (1988). Precipitation and atmospheric circulation anomaly patterns in the South American sector. *Revista Brasileira de Meteorologia*, Vol. 3, pp. 199-206.

Liebmann B. & Mechoso C. R. (2010). *The South American Monsoon System, Chapter 8 in The Global Monsoon System: Research and Forecast*, 2nd Edition. C. P Chang *et al*., (eds.) World Scientific Publishing: Singapore. 550 p.

Liebmann, B. & Marengo, J. A. (2001). The seasonality and interannual variability of rainfall in the Brazilian Amazon basin. *J. Climate*, Vol. 14, pp. 4308-4318.

Liebmann, B.; Kiladis, G.N., Vera, C.S., Saulo, A.C. & Carvalho, L.M.V. (2004). Subseasonal variations of rainfall in South America in the vicinity of the low-level jet east of the Andes and comparison to those in the South Atlantic convergence zone. *J. Climate,* Vol. 17, pp. 3829-3842.

Madden, R. & Julian, P. (1972). Description of global-scale circulation cells in the tropics with a 40-50 day period. *J. Atmos. Sci*., Vol. 29, pp. 1109-1123.

Madden, R. & Julian P. (1994). Observations of the 40-50 day tropical oscillation: A review. *Mon. Wea.Rev*., Vol. 112, pp.814-837.

Madden, R. A. & P. R. (1994). Observations of the 40-50-day tropical oscillation - A review. *Mon. Wea. Rev*., Vol. 122, pp. 814-837.

Marengo, J. A.; Liebmann, B., Kousky, V., Filizola, N. & Wainer I. (2001). On the onset and end of the rainy season in the Brazilian Amazon basin. *J. Climate*, Vol. 14, pp833-852.

Marengo, J. A.; Liebmann, B.; Grimm, A. M.; Misra, V.; Silva Dias, P. L.; Cavalcanti, I. F. A.; Carvalho, L. M. V.; Barbery, E. H.; Ambrizzi, T.; Vera, C. S.; Saulo, A. C.; Nogues-Paegle, J.; Zipser, E.; Seth, A. & Alves, L. M. (2010). Review: Recent developments on the South American monsoon system. *Int. J. Climatol.,* DOI: 10.1002/joc.2254

Markham, C. G. & McLain, D. R. (1977). Sea Surface temperature related to rain in Ceara, northeastern Brazil. *Nature*, Vol.265, pp. 320-325.

Mossman, R. C. (1924). Indian Monsoon rainfall in relation to South America weather. *Mem. Ind. Meteor. Dept*, Vol. 23, pp. 157-242.

Moura, A. D. & Shukla, J. (1981). On the dynamics of droughts in northeast brazil: observations, theory and numerical experiments with a general circulation model. *J. Atmos. Sci.*, Vol. 38, pp. 2653–2675. doi: 10.1175/1520-0469(1981)038<2653:OTDODI>2.0.CO;2

Negri, A. J.; Xu, L. & Adler, R. F. (2002). A TRMM-calibrated infrared algorithm applied over Brazil. J. Geophys. Res., 107(D20), 8048, doi:10.1029/2000JD000265.

Nieto-Ferreira, R. & Rickenbach, T. M. (2010). Regionality of monsoon onset in South America: A three-stage conceptual model. *Int. J. Climatol.*, DOI:10.1002/joc.2161.

Nobre, P. & Srukla, J. (1996).Variations of Sea Surface Temperature, Wind Stress, and Rainfall over the Tropical Atlantic and South America. *J. Climate*, Vol. 9, pp. 2464–2479. doi: 10.1175/1520-0442(1996)009<2464:VOSSTW>2.0.CO;2

Nogues-Paegle, J. & Mo, K. C. (1997). Alternating wet and dry conditions over South America during summer. *Mon Wea. Rev.*, Vol. 125, pp. 279-291.

Nogues-Paegle, J. & Coauthors, (2002). Progress in Pan American CLIVAR Research: Understanding the South American Monsoon. *Meteorologica*, Vol. 27, pp. 3-32.

Onogi, K. & Coauthors, (2005). Japanese 25-year reanalysis project - Progress and status. *Quart. J. Roy. Meteor. Soc.*, Vol. 131, pp. 3259-3268.

Onogi, K. & Coauthors (2007). The JRA-25 reanalysis. *J. Meteor. Soc. Japan*, Vol. 85, pp. 369-432.

Raia, A. & Cavalcanti, I. F. A. (2008). The Life Cycle of the South American Monsoon System. *J. Climate*, Vol. 21, pp. 6227–6246. doi: 10.1175/2008JCLI2249.1

Rienecker, M.M.; Suarez, M.J., Gelaro, R., Todling, R., Bacmeister,J., Liu, E., Bosilovich, M.G., Schubert, S.D., Takacs, L., Kim, G.-K., Bloom, S., Chen, J., Collins, D., Conaty, A., da Silva, A., et al., 2011. MERRA - NASA's Modern-Era Retrospective Analysis for Research and Applications. *J. Climate*, Vol. 24, 3624-3648, doi: 10.1175/JCLI-D-11-00015.1.

Ropelewski, C. F. & Halpert, M. S. (1987). Global and regional scale precipitation patterns associated with the El Niño-Southern Oscilation. *Mon. Wea. Rev.,* Vol. 115, pp. 1606-1626.

Ropelewski, C. F. & Halpert, M. S. (1989). Precipitation Patterns Associated with the High Index Phase of the Southern Oscillation. *J. Climate*, Vol. 2, pp. 268–284.

Saha, S., & Coauthors (2010). The NCEP Climate Forecast System Reanalysis. Bull. *Amer. Meteor. Soc.*, Vol. 91, pp. 1015–1057.

Servain, J. (1991). Simple Climatic Indexes for the Tropical Atlantic Ocean and some applications. *Journal of Geophysical Research-Oceans*, Vol. 96(C8), pp. 15137-15146.

Silva, A. E. & Carvalho, L. M. V. (2007). Large-scale index for South America Monsoon (LISAM). *Atmospheric Science Letters* 8: pp. 51–57.

Silva Dias, P. L., Bonatti, J. P. & Kousky, V. E. (1987). Diurnally Forced Tropical Tropospheric Circulation over South America. *Mon. Wea. Rev.*, Vol. 115, pp. 1465–1478.

Silva, V. B. S. & Kousky, V. E. (2001). Intraseasonal precipitation variability over eastern Brazil during the summer of 1991–2000 (in Portuguese). *Rev. Bras.Meteorol*. Vol. 16, pp. 187–199.

Silva, V. B. S.; Kousky, V. E. & Busalacchi, A. J. (2005). CLIVAR Science: Application to energy - The 2001 Energy Crisis in Brazil, *CLIVAR Exchanges*, Vol. 10, No.2.

Silva, V. B. S. & Berbery, E. H. (2006). Intense Rainfall Events Affecting the La Plata Basin. *J. Hydrometeor.*, Vol. 7, pp. 769–787. doi: 10.1175/JHM520.1

Silva, V. B. S.; Kousky, V. E., Shi, W. & Higgins, R. W. (2007. An Improved Gridded Historical Daily Precipitation Analysis for Brazil. J. Hydrometeor., Vol. 8, pp. 847-861.

Silva, V. B. S.; Kousky, V. E. & Higgins, R. W. 2011. Daily Precipitation Statistics for South America: An Intercomparison between NCEP Ranalyses and Observations. *J. Hydrometeor.*, Vol. 12, pp. 101-117.

Streten, N. A. (1983). Southern Hemisphere circulation contrasts in the winters of 1972 and 1973: *Preprints First International Conference on Southern hemisphere Meteorology., Sao Jose dos Campos, Brazil.*, 108-111.

Uppala, S. M. & Coauthors (2005). The ERA-40 re-analysis. *Quart. J. Rot. Meteor. Soc*., Vol. 131, pp.2961-3012.

Vera C. S.; Baez J., Douglas M., Emanuel C., Marengo J. A., Meitin J., Nicolini M., Nogues-Paegle J., Paegle J., Penalba O., Salio P., Saulo C., Silva Dias M. A. F., Silva Dias P. L. , Zipser E. (2006a). The South American Low-Level Jet Experiment. *Bulletin of the American Meteorological Society* 87: 63–77.

Webster, P. J. 1972. Response of the tropical atmosphere to local, steady forcing. *Mon. Wea. Rev*., Vol. 100, pp. 518-541.

Wheeler, M. & Hendon, H. (2004). An All-Season Real-Time Multivariate MJO Index: Development of an Index for Monitoring and Prediction. *Mon. Wea. Rev*., Vol. 132, pp. 1917-1932.

Zhang, C. (2005). Madden-Julian Oscillation. *Reviews of Geophysics*, Vol. 43, pp. 1-36.

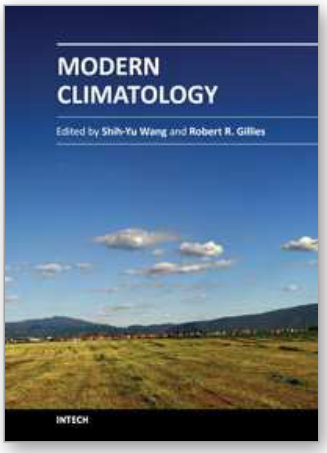

Modern Climatology

Edited by Dr Shih-Yu Wang

ISBN 978-953-51-0095-9

Hard cover, 398 pages

Publisher InTech

Published online 09, March, 2012

Published in print edition March, 2012

Climatology, the study of climate, is no longer regarded as a single discipline that treats climate as something that fluctuates only within the unchanging boundaries described by historical statistics. The field has recognized that climate is something that changes continually under the influence of physical and biological forces and so, cannot be understood in isolation but rather, is one that includes diverse scientific disciplines that play their role in understanding a highly complex coupled "whole system" that is the earth's climate. The modern era of climatology is echoed in this book. On the one hand it offers a broad synoptic perspective but also considers the regional standpoint, as it is this that affects what people need from climatology. Aspects on the topic of climate change - what is often considered a contradiction in terms - is also addressed. It is all too evident these days that what recent work in climatology has revealed carries profound implications for economic and social policy; it is with these in mind that the final chapters consider acumens as to the application of what has been learned to date.

How to reference

In order to correctly reference this scholarly work, feel free to copy and paste the following:

Viviane B. S. Silva and Vernon E. Kousky (2012). The South American Monsoon System: Climatology and Variability, Modern Climatology, Dr Shih-Yu Wang (Ed.), ISBN: 978-953-51-0095-9, InTech, Available from: http://www.intechopen.com/books/modern-climatology/the-south-american-monsoon-system-climatology-and-variability

INTECH
open science | open minds

InTech Europe
University Campus STeP Ri
Slavka Krautzeka 83/A
51000 Rijeka, Croatia
Phone: +385 (51) 770 447
Fax: +385 (51) 686 166
www.intechopen.com

InTech China
Unit 405, Office Block, Hotel Equatorial Shanghai
No.65, Yan An Road (West), Shanghai, 200040, China
中国上海市延安西路65号上海国际贵都大饭店办公楼405单元
Phone: +86-21-62489820
Fax: +86-21-62489821